Scottish Government
Riaghaltas na h-Alba
gov.scot

Developing marine mammal Dynamic Energy Budget models and their potential for integration into the iPCoD framework

Scottish Marine and Freshwater Science Vol 11 No 11

J Harwood, C Booth, R Sinclair and E Hague

marinescotland

Developing marine mammal Dynamic Energy Budget models and their potential for integration into the iPCoD framework

Scottish Marine and Freshwater Science Vol 11 No 11

John Harwood, Cormac Booth, Rachael Sinclair and Emily Hague

Published by Marine Scotland Science

ISSN: 2043-7722
DOI: 10.7489/12328-1

Marine Scotland is the directorate of the Scottish Government responsible for the integrated management of Scotland's seas. Marine Scotland Science (formerly Fisheries Research Services) provides expert scientific and technical advice on marine and fisheries issues. Scottish Marine and Freshwater Science is a series of reports that publishes results of research and monitoring carried out by Marine Scotland Science. It also publishes the results of marine and freshwater scientific work carried out for Marine Scotland under external commission. These reports are not subject to formal external review.

This report presents the results of marine and freshwater scientific work carried out for Marine Scotland under external commission.

Contents

Figures

Tables

Developing marine mammal Dynamic Energy Budget models and their potential for integration into the iPCoD framework

John Harwood, Cormac Booth, Rachael Sinclair and Emily Hague

Executive Summary

Bioenergetic models have been used to infer changes in an individual's energy stores with behavioural state or as a consequence of disturbance, and have been widely used to investigate potential impacts of disturbance on marine mammals at both individual and population level. Dynamic Energy Budget (DEB) theory provides a mechanistic framework that predicts the consequences of an organism's acquisition of environmental resources for energy demanding traits, such as growth and reproduction, via internal physiological functions. The equations in a DEB model describe the life history processes of a cohort of organisms, based on energy fluxes. Resources assimilated from the environment are allocated to maintenance, growth and reproduction via a reserve compartment. The overall objective of this project was to explore how DEB frameworks can be used to model the link between disturbance and population vital rates for five UK species of marine mammal to potentially improve marine mammal assessments for offshore renewable developments.

The report describes in detail the different parameters that are required by a DEB model, which of those are likely to be found in or derived from the literature and which are unknown and require subjective judgement. Based on an extensive literature search, we provide suggested parameter values for harbour porpoise, bottlenose dolphins, minke whales, harbour seals and grey seals in the UK, noting in each case the literature that was used to derive the parameter and where they were estimated by subjective expert judgement. While recommended parameters were collated for each of the five species, a full DEB model was created for harbour porpoise only. Therefore, the focal species in this report is the harbour porpoise. The text details the results of the literature search for harbour porpoise and exactly how each parameter value was calculated or estimated. Similar detail is provided for bottlenose dolphins, minke whales, harbour seals and grey seals in Appendix 1-4.

Where values required subjective expert judgement or where a range of values are estimated in the literature, sensitivity testing was conducted to understand the sensitivity of the DEB model to plausible ranges of these parameters. Sensitivity

testing showed that varying the age at which the calf's foraging efficiency is 50% made significant changes to calf survival and consequential reproductive success.

The report then illustrates how the DEB model can be used to investigate the potential effects of disturbance that causes a reduction in energy intake and subsequent effect on vital rates (individual survival and birth rate), using harbour porpoise as an example. The scenarios explored here used a theoretical assumption that an individual's energy intake would be reduced by 25% on the day it was disturbed. The effect of this disruption, experienced during different time periods in the year, when females are in different reproductive stages was investigated. The model highlighted that nursing female harbour porpoise are particularly susceptible to disturbance between the time the calf is born until it is able to acquire at least some food independently. The results showed that disturbance after the mother has begun to reduce milk provisioning and post-weaning is unlikely to markedly affect survival rates.

Finally, the report explores if DEB models could potentially be integrated into the interim PCoD model to replace the dependency on transfer functions derived using expert elicitation approaches that are currently used to the links between disturbance and subsequent effect on vital rates. One potential issue with this approach is that some of the parameters which potentially have a large effect on susceptibility to disturbance cannot be measured directly and, therefore, have to be chosen subjectively. There is, therefore, a requirement for experts to agree on plausible ranges for the relevant model parameters; however, once these are agreed, the incorporation of DEB models into the iPCoD code can be done without major structural changes.

Introduction

Using bio-energetics models to understand PCoD

Disturbance can cause behavioural, physiological and health changes which can have subsequent effects on an individual's vital rates, such as survival and reproduction. The cost of disturbance is in most cases mediated by the state of the individual (e.g. life history stage, exposure history), and the environment that the individual is in (e.g. resource availability). By modelling health, we have an explicit scalar link between individual health, response to disturbance, and the consequential population demographic effects of this disturbance (Pirotta et al., 2018a). To date, many PCoD studies have used only changes in an individual's energy stores (e.g. body condition) as a proxy metric of health (Schick et al., 2013; Nabe-Nielsen et al., 2014; New et al., 2014; Villegas-Amtmann et al., 2015; McHuron et al., 2017; Villegas-Amtmann et al., 2017; Nabe-Nielsen et al., 2018; Pirotta et al., 2018b). To build on this, bioenergetics models also consider the variance in energetic demands on an individual and their associated behavioural and physiological state during different life history stages and take into account the state of the environment the individual is in (e.g. resource density, presence of predators). Marine mammals show a variety of life history patterns across the taxa, with a spectrum of reproductive strategies between the 'capital breeding' end (e.g. humpback whale, grey seal) through to the 'income breeding' end (e.g. bottlenose dolphin, harbour seal). The choice of reproductive strategy can have a great impact on the energetic consequences of disturbance, varying each individual's vulnerability to disturbance based on both its reproductive strategy and stage. Accounting for life history stage and the associated energetic demands in PCoD models means the model can account for how these demands might affect the individual's response to disturbance. An example of variation in disturbance response based on context would be that a lactating female in a resource poor environment would likely respond very differently to a non-lactating female in a resource-rich environment (Hin et al., 2019).

Bioenergetic models have been used to infer changes in an individual's energy stores with behavioural state or as a consequence of disturbance (see Table 1 for a comprehensive list of examples), and have been widely used to investigate potential impacts of disturbance (both natural and anthropogenic) on marine mammals at both individual and population level (see Pirotta et al., 2018a for a review). However, many bioenergetic models assess the effects of disturbance on marine mammals by focusing on a single reproductive cycle of a females life history (Braithwaite et al., 2015; Christiansen and Lusseau, 2015; Villegas-Amtmann et al., 2015; McHuron et

al., 2016; Pirotta et al., 2018c). For an in-depth assessment of how disturbance might affect population growth rate over a longer period, it is necessary to model female energetics over the entire lifespan, in order to highlight life history stages that are particularly vulnerable to disturbance (Villegas-Amtmann et al., 2017; McHuron et al., 2018; Pirotta et al., 2018a). Hin et al. (2019) used the Dynamic Energy Budget model presented by De Roos et al. (2009) as a baseline model to simulate the life history of a female pilot whale from weaning age onwards (including during pregnancy and lactation), and for a calf from birth until weaning. Incorporation of this DEB model into a PCoD framework allowed the authors to predict how vulnerability to different disturbances varied with resource availability and life history stage.

Table 1

Examples of recent bio-energetic models developed for marine mammals.

Reference	Species	Summary
		Cetaceans
Christiansen and Lusseau (2015)	Minke whale	Mechanistic model to measure the effects of behavioural disturbances caused by whale watching activities on foetal growth.
Farmer et al. (2018)	Sperm whale	Stochastic life-stage structured bioenergetic model to evaluate the consequences of reduced foraging efficiency on carbohydrate, lipid, and protein reserves in the blubber, muscle, and viscera.
Noren (2011)	Killer whale	Body mass, field metabolic rate (FMR), and daily prey energy requirements (DPERs) were estimated. FMRs of adults were also calculated from resident killer whale activity budgets and the metabolic cost of swimming at speeds associated with daily activities.
Villegas-Amtmann et al. (2017)	Gray whale	Female bioenergetics model to examine potential consequences of energy lost from foraging cessation caused by anthropogenic disturbance.
Villegas-Amtmann et al. (2015)	Gray whale	Bioenergetics model to determine energy requirements for a two-year reproductive cycle and determined the consequences of lost energy under three possible disturbance scenarios.
Pirotta et al. (2018b)	Blue whale	Dynamic state variable model developed to explore the effects of environmental and anthropogenic perturbations on female reproductive success.
Pirotta et al. (2019)	Blue whale	Dynamic state variable model to predict the effects of changing environmental conditions and increasing human disturbance on the population's vital rates, particularly on female survival and reproductive success.

Hin et al. (2019)	Pilot whale	Bioenergetic model covering the complete life cycle of a female. The expected lifetime reproductive output of a single female can then be used to predict the level of disturbance that leads to population decline.
Gallagher et al. (2018)	Harbour porpoise	Velocity-dependent bioenergetic model to estimate potential food requirements. This varied by the energetic cost of basal metabolism, locomotion, thermoregulation and reproduction.
Srinivasan et al. (2018)	Bottlenose dolphin	Use spatially explicit individual based models to investigate how changes in lactation state and the environment (predation risk) affect behaviour and the associated energetic costs in bottlenose dolphins.
Spitz et al. (2018)	Harbour porpoise, Common dolphin, Striped dolphin, Bottlenose dolphin, Long-finned pilot whale, Risso's dolphin, Sperm whale, Cuvier's beaked whale, Minke whale and Fin whale	Used Monte Carlo resampling methods to estimate annual and seasonal consumption of prey. Also assessed energy requirements of each species.
		Pinnipeds
McHuron et al. (2016)	Pinniped(s)	Framework using state-dependent behavioural theory implemented by Stochastic Dynamic Programming. Examined how disturbance affected pup recruitment separately for each reproductive strategy, and the impact of foraging decisions and parameter values on model results.
Beltran et al. (2017)	Weddell seal	Agent-based, ecophysiological model that simulates the energy balance of adult female Weddell seals.
McHuron et al. (2017)	California sea lion	Bioenergetic model to quantify the energy and prey requirements of adult females. Examined how changes in at-sea field metabolic rates and the proportion of time at sea affected energy requirements.
McHuron et al. (2018)	California sea lion	Developed a method using state-dependent behavioural theory implemented via Stochastic Dynamic Programming (SDP) for predicting the population consequences of disturbance on the physiology and reproductive behaviour.
Pirotta et al. (2018c)	Northern elephant seal	Bayesian state-space model that concurrently estimates an individual's location, feeding activity, and changes in condition. Demonstrates how the model can be used to simulate realistic patterns of disturbance at different stages of the trip, and how the predicted accumulation of lipid reserves varies as a consequence.

Goedegebuure (2018); Goedegebuure et al. (2018)	Southern elephant seal	Built individual based models coupled with dynamic energy budget models. Simulated energy use and life histories.

An introduction to DEB models

Dynamic Energy Budget (DEB) theory (Nisbet et al., 2000; Kooijman and Kooijman, 2010) provides a mechanistic framework that predicts the consequences of an organism's acquisition of environmental resources for energy demanding traits, such as growth and reproduction, via internal physiological functions. DEB models employ a set of differential or difference equations and parameters that are based on unifying metabolic theory and can theoretically be used to model any species. These equations describe the life history processes of a cohort of organisms, based on energy fluxes. Resources assimilated from the environment are allocated to maintenance, growth and reproduction via a reserve compartment. In the standard DEB model, both structure and reserves contribute to total biomass, but only structure requires maintenance and all metabolic processes are fuelled from reserves. These two state variables (structure and reserves) can be difficult to measure directly in many species, but they can be linked to more easily observable traits such as body size or age at first reproduction.

According to Jager et al. (2016), DEB theory is "the best-tested and most comprehensive theory for the energy budget of organisms". The 'add my pet' database[1] contains details of more than 1,000 DEB models for different organisms. DEB models are widely used to investigate interactions between populations of organisms and their resources (e.g. De Roos et al., 2009), but they have also been used to investigate the toxic effects of chemical stressors. This latter approach (known as DEBtox[2]), uses the concept of physiological modes of action that "summarizes how a stressor affects parameters associated with processes involving energy acquisition and use" (Murphy et al., 2018b). This is achieved by coupling a standard DEB model to toxicokinetic (TK) models that describe the processes of bioaccumulation, elimination and transformation within and organism, and toxicodynamic (TD) models that describe how the chemical affects particular biological targets (Murphy et al., 2018b). Interestingly, the first DEB model developed for a marine mammal species (Klanjscek et al., 2007) includes a TK sub-model for the accumulation of lipophilic toxicants (such as PCBs) and their transmission to offspring.

[1] http://www.bio.vu.nl/thb/deb/deblab/add_my_pet/index.html

[2] https://leanpub.com/debtox_book

Murphy et al. (2018b) and Murphy et al. (2018a) have described how the DEBtox approach could be expanded to model the action of (and interaction between) a much wider range of stressors. This would involve the use of models based on the adverse outcome pathway (AOP) framework that describe the effect of stressors on cellular endpoints that may have consequences for energy acquisition and expenditure. The AOP framework is widely used to assess the potential risks to human health from newly-synthesized chemicals. Murphy et al. (2018b) and Murphy et al. (2018a) suggest that these AOP models could be linked to a DEB model for a particular organism via the damage that the modelled stressors might cause to cells, organs or the whole animal. Such hybrid models could then be used to predict the population-level consequences of exposure to multiple stressors.

DEB models for marine mammals

In many marine mammal species, subcutaneous blubber appears to act as their main energy reserve. The size of this reserve can be estimated directly from dead or sacrificed animals by dissecting out the tissue and weighing it (e.g. Worthy and Lavigne, 1987). In can be estimated indirectly using hydrogen isotope dilution techniques (e.g. Costa et al., 1986), although this technique provides an estimate of total body lipid, rather than just blubber. However, blubber performs a number of other functions in marine mammals: it insulates; adjusts buoyancy; defines body shape and streamlines; and acts as a spring (Koopman, 2007). In addition, the blubber of beaked whales and sperm whales is largely composed of waxy esters, which are much more difficult to catabolise than the fatty acids that are the main component of most other species' blubber. As a result, individual marine mammals may not be able to use all of the lipid stored in blubber as an energy reserve without compromising their survival.

The most detailed information on the way in which marine mammals manage their energy reserves comes from studies of fasting seals. Although >90% of the energy required by fasting northern elephant seal, harp seal and grey seal pups comes from the catabolism of lipids (Worthy and Lavigne, 1987; Noren et al., 2003; Bennett et al., 2007), they also obtain energy from the catabolism of lean body tissue. In fact, the decrease in their lean body mass may actually exceed the decrease in the size of their lipid reserves, because lean tissue is mostly comprised of water (Noren et al., 2003). Blubber may be preferentially mobilized if ambient water temperature increases, thus reducing the need for extra insulation (e.g. as documented in fasting harbour seal pups by Muelbert and Bowen, 1993). Similarly, lactating females may

preferentially catabolize blubber lipids to provide the energy and raw materials for milk production (Costa et al., 1986).

To date, four DEB models for marine mammals have been published. Klanjscek et al. (2007) developed a DEB model for right whales (*Eubalaena* spp.). Although their primary concern, as noted above, was to understand the factors that might affect the bioaccumulation of lipophilic toxicants, the same model structure could be used to investigate the effects of disturbance that reduced daily energy intake on reproduction and calf survival. Goedegebuure et al. (2018) developed a DEB model for southern elephant seals (*Mirounga leonina*) and used it to examine the potential effects of changes in resource availability on breeding success and juvenile survival.

Hin et al. (2019) developed a DEB model for North Atlantic long-finned pilot whales (*Globicephala melas*), which they used to investigate the effects of disturbance that resulted in reduced energy intake on lifetime reproductive success (i.e. fitness). A subsequent manuscript (Hin et al., in review) expands this model to consider the effect of density dependence. Hin et al. (2019) found that the calves of females breeding for the first time were particularly sensitive to disturbance, but that all calves – and even lactating females – were at risk as the duration of disturbance increased. Moretti (2019) adapted Hin et al.'s model for Blainville's beaked whale (*Mesoplodon densirostris*) and used this model to investigate the potential population consequences of changes in foraging behaviour resulting from exposure to navy sonars. In addition, outputs from DEB models developed for harbour porpoise and Pacific walrus (*Odobenus rosmarus*) have been used to inform expert elicitations for these species (Booth et al., 2019; Harwood et al., 2019).

Report intent

The overall objective of this project is to explore how DEB frameworks can be used to model the link between disturbance and population vital rates for five UK species of marine mammal (harbour porpoise, bottlenose dolphin, harbour seal, grey seal and minke whale) to help improve marine mammal assessments for offshore renewable developments.

Parameterising DEB models for the 5 iPCoD species

Booth et al. (2019), Harwood et al. (2019) and Moretti (2019) all used the same formulation as Hin et al. (2019) for their marine mammal DEB models. We suggest that this formulation is also appropriate for the five marine mammal species modelled

in the iPCoD software. In this section, we describe the parameters and functions of the model and discuss how they can be estimated for the iPCoD species.

The Hin et al. (2019) model tracks the way in which individual female marine mammals assimilate energy over the course of their lives from weaning to death, and how this energy is allocated to field metabolism, growth, foetal development, and lactation. If assimilated energy on a particular day exceeds the energy required for these activities, the surplus energy is stored in a reserve compartment (De Roos et al., 2009; Kooijman and Kooijman, 2010), primarily – but not exclusively - as fat tissue around internal organs and as blubber. If energy expenditure exceeds energy assimilation, the balance is provided by catabolizing reserve tissue. The model also tracks these energy fluxes up to the age at weaning for every calf that a female produces. In this way, it is possible to use the expected lifetime reproductive output of each simulated female to examine the population consequences of different conditions (including a changing environment and/or the effects of disturbance). The original model was cast as a set of differential equations and operates in continuous time. To speed calculation, we have recast the model as a set of differential equations with a time step of one day.

Individual females are characterized by their age (a in days), structural size (length, La and core body mass Sa). Reserve mass (F_t) will vary over time (t) depending on the activity and state of each individual. Total mass on a particular day (W_t) is therefore equal to $(Sa + F_t)$, and maintenance mass $MM_t = S_t + \Theta_F F_t$, where Θ_F accounts for the different costs of maintaining core tissue and reserves. Relative body condition (ρt) – henceforth referred to simply as 'body condition' - on day t is defined as reserve mass/total body mass (F_t / W_t).

Females can be in one of four states:

- 'resting' (i.e. neither pregnant nor lactating, this includes the juvenile period from weaning to first conception);
- 'pregnant (but not lactating)';
- 'lactating (but not pregnant)'; and
- 'lactating & pregnant'.

Individual energy flux is assumed to depend on resource density (R) and the state of the individual.

Although the Hin et al. (2019) model has a large number of parameters, many of these can be estimated using values from the peer-reviewed literature. However,

others require some subjective judgement. In the following sections, we first describe the parameters whose values can be estimated directly from the literature. We then describe the parameters whose values must be chosen by the model builder. Finally, we review the published information that can be used to provide parameter values for bottlenose dolphins, minke whales, harbour seals, and grey seals. Parameter values for harbour porpoise are discussed below. Throughout, we use the parameter symbols and names from Tables 1 and S1 – in Hin et al. (2019).

Estimable parameters of the Hin et al. (2019) DEB model

Gestation period (T_P) This is usually estimated from a combination of estimates of foetal growth rate and mean length at birth, using the assumption that foetal growth is approximately linear (Perrin and Reilly, 1984).

Lactation period/age at weaning (T_L) Perrin and Reilly (1984) provide a review of the methods used to determine lactation period and age at weaning. These include estimates of the ratio of lactating to pregnant animals in a sample of mature females, estimates of the age of the largest calf observed associating with a female, stomach content analysis, and behavioural observations.

Structural length and structural mass (ω_1, ω_2) Most marine mammal DEB models have used a von Bertalanffy growth curve to describe changes in La with age, and then converted length to mass using a simple power function (e.g. $S_a = \omega_1.L_a{}^{\omega_2}$). However, there is no requirement to use this approach, and any empirically derived relationship between weight and age can be used in the model.

Field metabolic maintenance scalar (σ_M) The Hin et al. (2019) model assumed that an individual's field metabolic rate is a simple multiple of the value predicted by the Kleiber (1975) relationship (i.e. $K.MM_t^{0.75}$, where K = 0.294 MJ·kg^{-1}.day^{-1}). Estimates of this parameter can be obtained from respirometry studies of captive animals (e.g. Worthy and Lavigne, 1987; Sparling et al., 2006), or they may simply be assumed. For example, Hin et al. (2019) used a value of 0.75 for $\sigma_M.K$ based on Lockyer (1993) assumption that the field metabolic rate for pilot whales is 2.5x their resting metabolic rate.

Energetic cost per unit structural mass (σ_G) This is the amount of energy required to produce 1 kg of tissue (i.e. the energetic content of the new tissue and the energetic overheads required to produce it). Hin et al. (2019) obtained an indirect estimate of σ_G = 30 MJ.kg^{-1} from the Brody (1968) formula for the heat of gestation and the Lockyer (1993) estimate of the energy density of pilot whale calf tissue.

However, direct measurements of this cost can be obtained from captive animals (e.g. Noren et al. (2014) for Pacific walrus).

Relative cost of maintaining reserves (Θ_F) According to DEB theory, reserve mass does not require any maintenance (i.e. $\Theta_F = 0$). However, the large lipid reserves maintained by most marine mammal species probably do incur additional costs in terms of drag and buoyancy. Hin et al. (2019) set Θ_F to 0.2 in order to account for these costs.

Reserve thresholds (ρ, ρ_s) In the Hin et al. (2019) model the rate of energy assimilation on a particular day (see below) is affected by an individual's current body condition (ρt) relative to the **target body condition** (ρ). That target condition is rarely – if ever – achieved in simulations. It is tempting to simply set ρ to the maximum recorded blubber: total body mass ratio for a particular species. However, captive harbour porpoises show strong seasonal variations in blubber thickness and total mass (Lockyer et al., 2003; Kastelein et al., 2019), which are closely correlated with water temperature and probably reflect a requirement for less insulation in summer. This suggests that ρ may vary seasonally, and we have included this provision in the DEB model for harbour porpoises described below.

The starvation body condition threshold (ρ_s) Represents the point at which further reduction in body condition is likely to have a negative effect on survival. It can be estimated from the ratio of blubber: total body mass of dead or dying animals that exhibit symptoms of terminal starvation (Kastelein and Van Battum, 1990; Koopman et al., 2002).

Catabolic efficiency of reserve conversion (ε-) The amount of energy produced by metabolising 1 kg of reserve tissue. It can be calculated from measurements of the changes in mass of fasting animals and estimates of their metabolic requirements during that fast (Muelbert and Bowen, 1993; Bennett et al., 2007).

Anabolic efficiency of reserve conversion (ε_+) The amount of energy required to produce 1 kg of reserve tissue. Since anabolism is likely to be less efficient than catabolism, Hin et al. (2019) used a value for ε_+ that was ~40% higher than ε-. However, it may be possible to estimate this parameter from measurements of the amount of additional food consumed by captive animals that have experienced fasting. For example, Kastelein et al. (2019) report that fasted, captive harbour porpoises recovered their original body weight within two days when they were offered twice the normal amount of food on those days. Estimates of the actual

amount of additional energy consumed by these animals could be used to calculate ε_+.

Efficiency of conversion of mother's reserves to calf tissue (σ_L) This parameter combines the efficiency with which a female converts ingested or reserve energy to milk and the assimilation efficiency of the calf. Lockyer (1993) assumed that efficiency of milk assimilation is 95% and that the efficiency of milk production in the mammary gland is 90%. Combining these estimates yields a value of 0.86, which was used by Hin et al. (2019) and may also be useful for other cetacean species. Direct estimation of this parameter should be possible from studies of energy transfer in lactating pinnipeds (e.g. Costa et al., 1986; Lang et al., 2011). For example, Fig. 3 of Costa et al. (1986) implies that conversion efficiency in northern elephant seals is close to 100%. However, it is not possible to calculate a precise value for σ_L from the results presented in this and other pinniped studies.

Age-dependent mortality rate Hin et al. (2019) calculated an age-varying mortality rate for pilot whales based on published estimates of age-specific survival rates. A similar procedure can be used to estimate this rate for the five iPCoD species from the age-specific survival rates provided in the iPCoD helpfile, or other published estimates (Winship, 2009; Arso Civil et al., 2018).

Other parameters of the DEB model

The parameters described in this section are difficult or impossible to estimate directly, and the modeller must choose appropriate values. However, this choice is not arbitrary because the range of feasible values for each parameter is often constrained by known features of the life history strategy of the species being modelled, as described below.

Resource density (R) To avoid having to account for differences among prey in energy density, catchability, and digestibility, and differences among individuals in their ability to assimilate energy, the Hin et al. (2019) model characterises the resources on which a species feeds in terms of the amount of assimilated energy they can provide to a female. Although it would be virtually impossible to measure resource density defined in this way, R provides a useful qualitative measure of environmental quality, with high resource density indicating high quality environments, and low resource density associated with poor environments. For simplicity, R is often assumed to be constant over time, but this can be easily modified – see Hin et al. (2019) for an example. R is the most important determinant of lifetime reproductive output (the number of female offspring raised to weaning in a

female's lifetime). It is, therefore, possible to choose an appropriate value for R based on what is known about the status of the population being modelled. For example, if the population is stable, R can be tuned so that lifetime reproductive success is 1.0.

Steepness of assimilation response (η) The amount of assimilated energy obtained from feeding each day depends on the resource density, the structural size of the animal to the power 2/3 (i.e. St(2/3), following Kooijman and Kooijman, 2010), and the individual's relative body condition (ρt). Individuals are assumed to assimilate energy at ½ of the maximum possible rate when their body condition is at the target body condition (ρ) and to increase their energy assimilation progressively if their body condition is reduced below the target value. This relationship also allows animals to compensate for the effect of lost foraging opportunities on their body condition by increasing energy assimilation on subsequent days, provided sufficient resources are available. Energy assimilation (I_t) on day t is described by:

$$I_t = \frac{R.S_t^{2/3}}{1 + e^{-\eta(\frac{\rho}{\rho t} - 1)}}$$

Figure 1 shows the effect of body condition relative to the target value ($\frac{\rho t}{\rho}$) and η on energy assimilation with η ranging from 5 to 25. The value of 15 used by Hin et al. (2019) is shown in bold. With higher values of η, energy assimilation is close to its maximum level over a wide range of value for ρt. Lower values of η result in a wider range of variation in energy assimilation with ρt. Information on how quickly fasting individuals that are in good condition recover the weight lost during the fast (e.g. Kastelein et al., 2019) could provide guidance as to a suitable value for η.

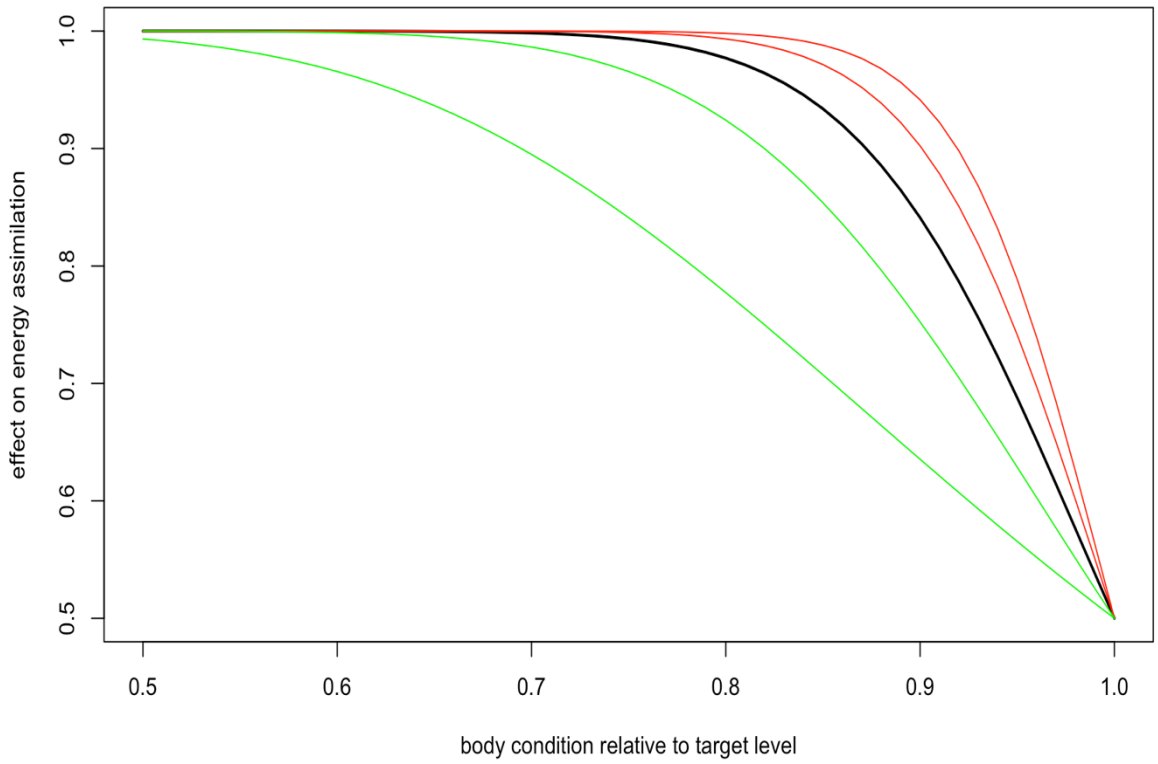

Figure 1: The effect of body condition relative to the target level ($\frac{\rho}{\rho t}$), and the steepness of the assimilation response (η) on energy assimilation as a proportion of its maximum rate. The relationship for η = 15 is shown in solid black. Curves in green are for values of η = 5 and 10; curves in red are for values of η = 20 and 25.

Effect of age on resource foraging efficiency (γ, T_R). This parameter takes account of the fact that newly-weaned calves will not be 100% efficient at foraging and that, for species with long lactation periods, calves may begin feeding during lactation. Its shape is controlled by T_R, the age at which a calf achieves a foraging efficiency that is 50% of an adult, and a shape parameter (γ) that determines how rapidly foraging efficiency approaches 100%. Figure 2 shows the effects of different values of γ on the shape of the function determining foraging efficiency. The value of γ = 3 used by Hin et al. (2019) is shown in bold. As an example, if T_R is one year, the function predicts that 100% foraging efficiency would be achieved by age five. Lower values of γ result in higher ages for 100% efficiency and higher values of γ result in lower ages for 100% efficiency. Although it may be possible to determine when calves begin feeding independently from an examination of stomach contents (e.g. Figure 3 in Muelbert and Bowen, 1993), direct estimation of these parameters is unlikely to be feasible. However, γ will affect post-weaning survival and age at first conception (see discussion of $F_{neonate}$ below). Independent information on current values for these demographic characteristics can therefore provide insights into the feasible range for this parameter.

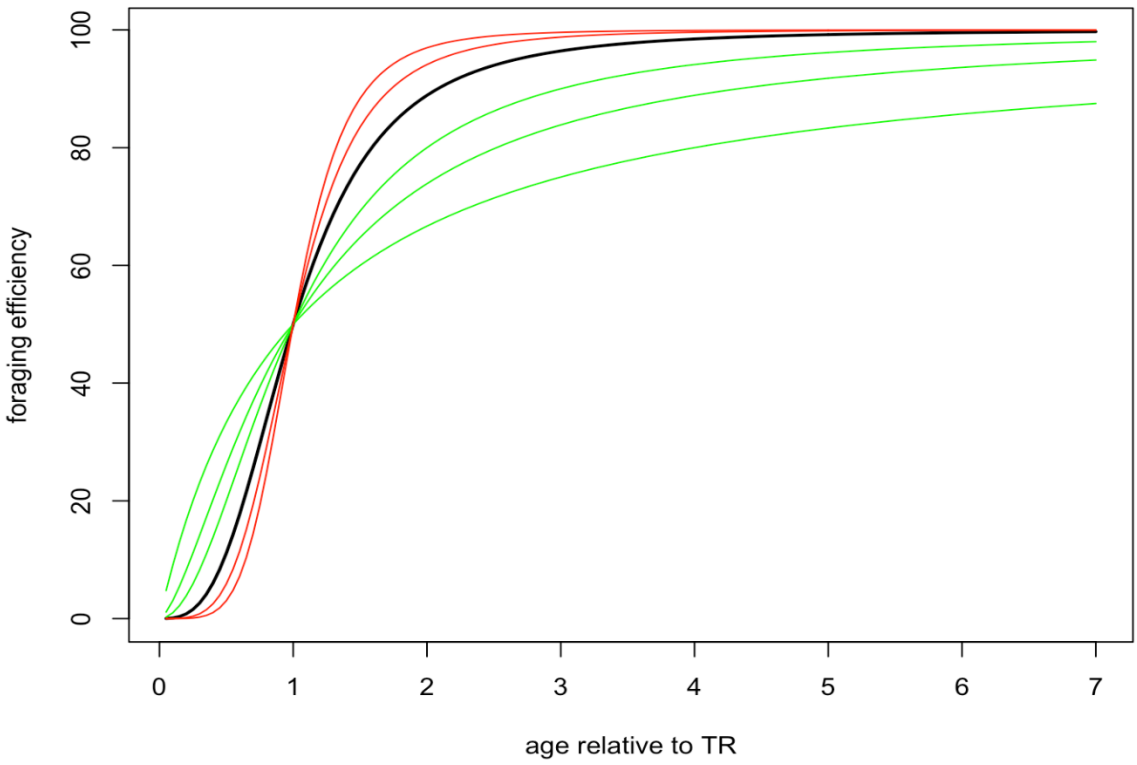

Figure 2: The effect of the shape parameter γ on the relationship between foraging efficiency and age (shown as a multiple of the age at which a calf achieves 50% foraging efficiency). T_R is one year. The curve for $\gamma = 3$ is shown in solid black. Green curves show the relationship for values of $\gamma < 3$; red curves represent values >3.

Starvation-induced mortality rate (μ_s) This parameter determines how long an individual is likely to survive if its body condition falls below the starvation body condition threshold (ρ_s). Probability of survival is modelled as:

$$\phi_t = e^{-\mu_s(\frac{\rho_s}{\rho_t}-1)}$$

Higher values of μ_s result in a lower probability of survival (Figure 3). Hin et al. (2019) used a value of 0.2, which implies that 50% of starving individuals will survive for one week if their body condition remains below the threshold.

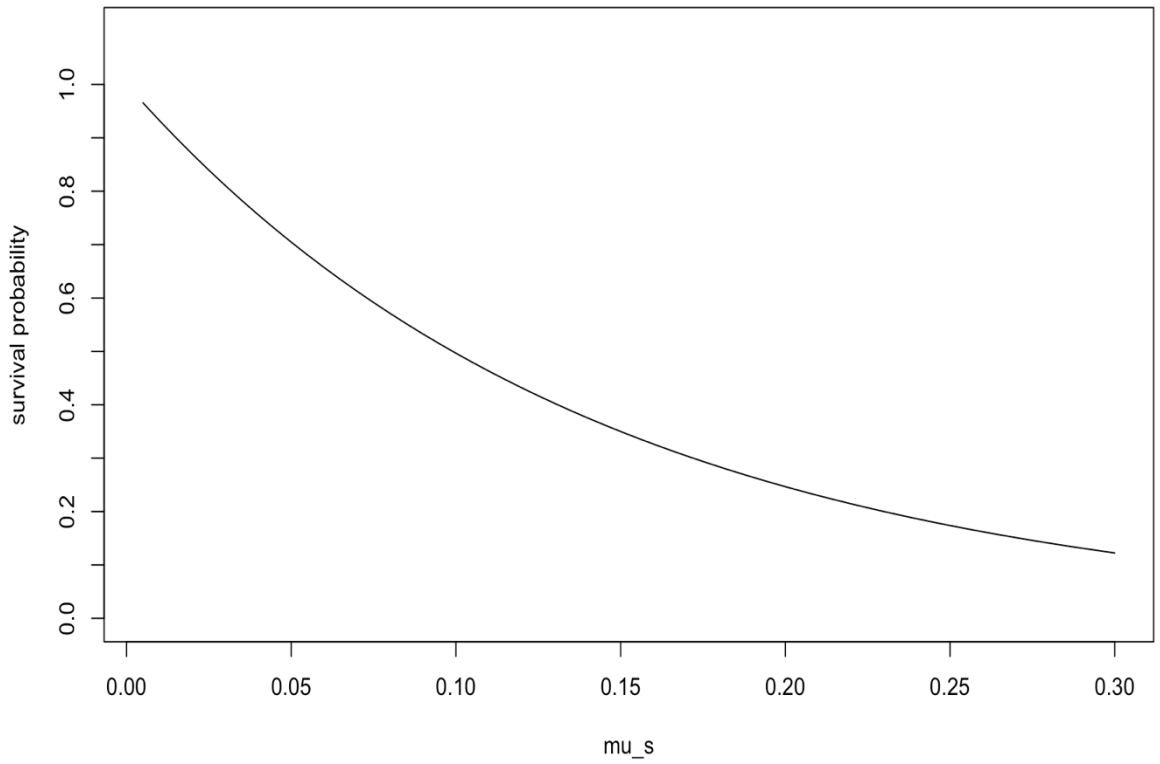

Figure 3: The effect of the starvation-induced mortality parameter (mu_s = μ_s) on the probability that an individual whose body condition has fallen to $\rho_s/2$ will survive for 1 week.

Pregnancy threshold ($F_{neonate}$) The Hin et al. (2019) model assumes that females can only become pregnant when the size of their reserves exceeds $F_{neonate}$. They used a value equivalent to the energetic costs of foetal growth and development plus the amount of reserves needed to avoid the onset of starvation for pilot whales, but other formulations have been used (e.g. for beaked whales – New et al., 2013). This effectively sets a minimum value for the age at first conception, because the absolute size of a female's reserves are determined by S_a and young females are too small to build up sufficient reserves, even if their foraging efficiency has attained its maximum level. Estimates of age at first conception are available from many marine mammal populations and these can be compared with predictions from the DEB model to provide a "reality check" on the appropriateness of the value chosen for $F_{neonate}$.

Effect of calf age on milk assimilation (T_N, ξ_C) Hin et al. (2019) proposed that females will provide all their calf's energy demands until the calf is T_N days old, and after this they will gradually reduce the amount of energy they supply according to the formula:

$$\left(1-\frac{(a-T_N)}{(T_L-T_N)}\right) \Big/ \left(1-\frac{\xi_C(a-T_N)}{(T_L-T_N)}\right)$$

Where a is calf age and T_L is age at weaning. Figure 4 shows the effect of the value of ξ_C on the shape of this relationship. For capital breeding species, such as many pinnipeds, which provide almost all of their pup's energy demands up until the age at weaning, T_N should be close to T_L and ξ_C will be close to one. Species, such as bottlenose dolphins, with an extended period of maternal care will have relatively small values of T_N and ξ_C.

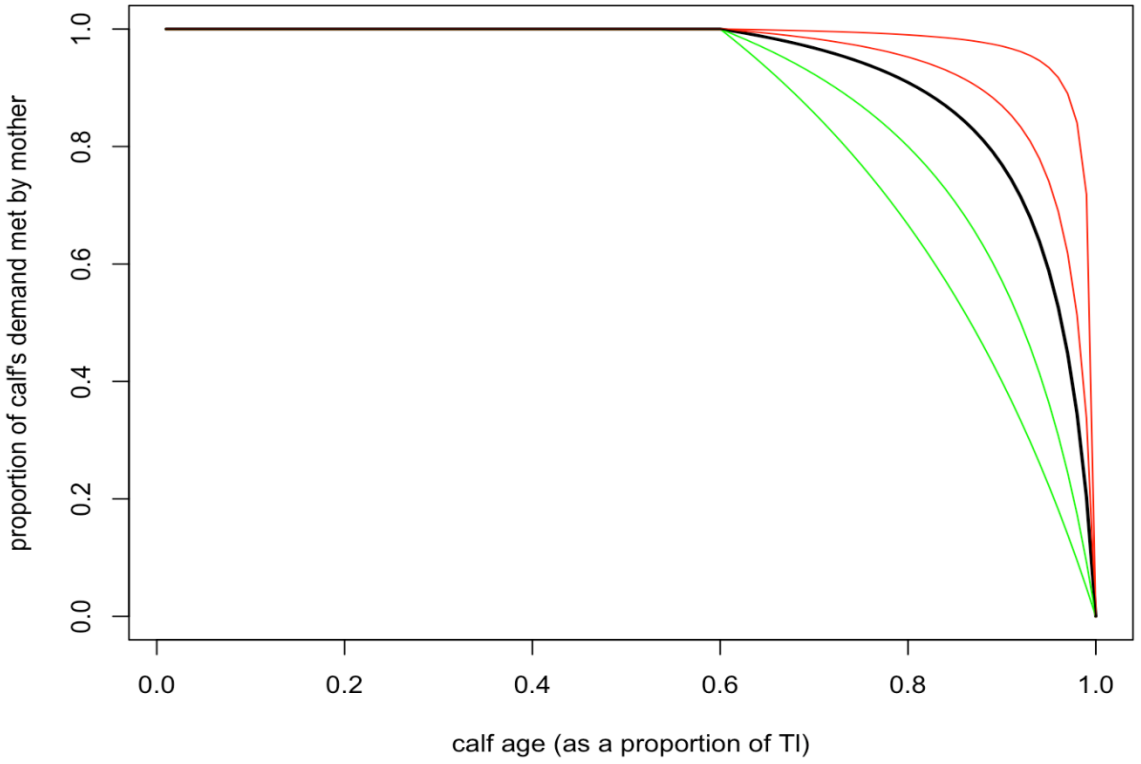

Figure 4: The effect of the non-linearity parameter ξ_C on the proportion of a calf's milk demand provided by its mother at different stages of lactation. T_N (the calf age at which the mother begins to reduce the amount of milk she supplies) was set at 60% of the duration of lactation (T_L). The solid black line shows the relationship for ξ_C = 0.9 (the value used by Hin et al. 2019). Green lines show the relationships for smaller values of ξ_C (0.5 and 0.75). Red lines show the relationship for larger values (0.95 and 0.99).

Effect of female body condition on milk provisioning (ξ_M) Hin et al. (2019) assumed that females will reduce the amount of milk they provide to their calf as their own body condition declines.

They used the function:

$$\frac{(1+\xi_M).(\rho_t-\rho_s)}{\{(\rho-\rho_s)+\ \xi_M.(\rho_t-\rho_s)\}}$$

to predict this reduction, where ρ_t is the female's body condition on day t, and ξ_M is described as the "non-linearity in female body condition-milk provisioning relation". Figure 5 shows how this shape of this relationship varies, depending on the value of ξ_M. Lower values of ξ_M represent a more conservative strategy, with females reducing the amount of milk they supply by 50% if their body condition falls below 60% of ρ if ξ_M = 0.5. Larger values reflect a strategy that is more "generous" to the calf. For example, if ξ_M = 10, body condition must be reduced close to ρ_s before milk supply is reduced by 50%.

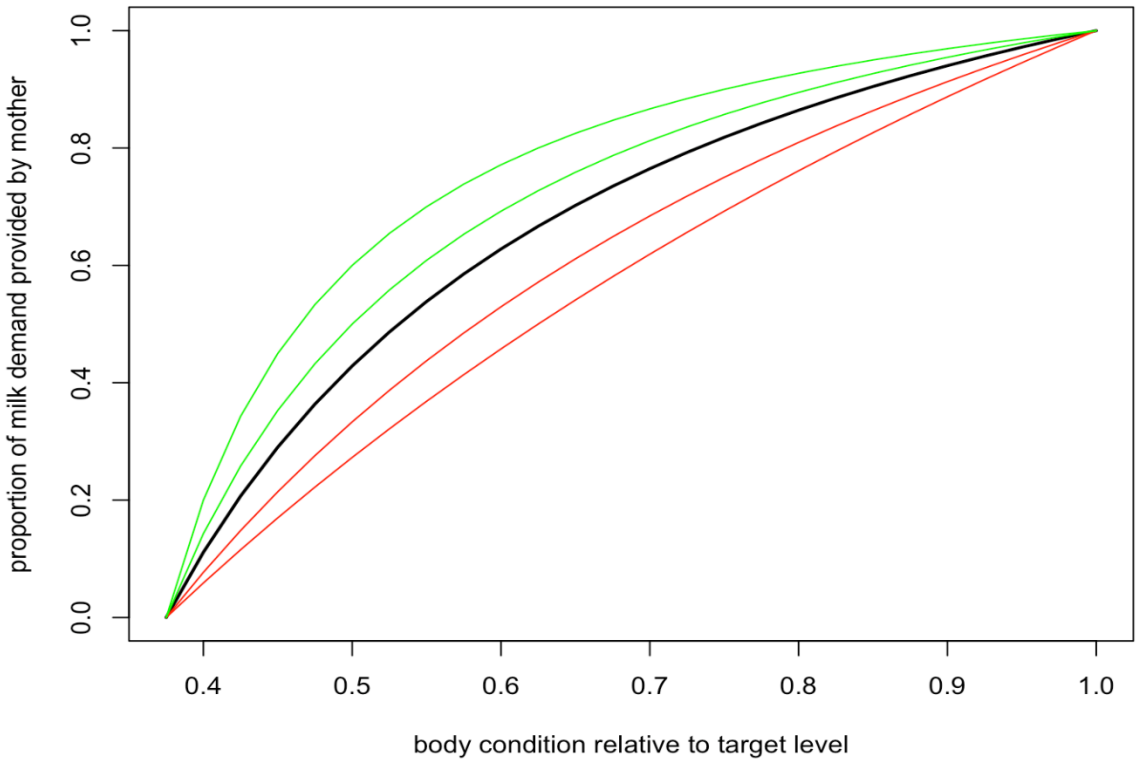

Figure 5: The effect of body condition relative to the target level ($\frac{\rho}{\rho t}$) of the female and the non-linearity parameter ξ_M on the proportion of a calf's milk demand provided by its mother. The solid black line shows the relationship for ξ_M = 2 (the value used by Hin et al. 2019). Green lines show the relationships for larger values of ξ_M (3 and 5). Red lines show the relationship for smaller values (0.5 and 1.0).

Lactation scalar (Φ_L) is analogous to R; because $\Phi_L.S_{c,t}^{2/3}$ determines the maximum amount of energy a calf can obtain from milk on day t, where $S_{c,t}$ is the structural mass of the calf on day t. Hin et al. (2019) estimated Φ_L for pilot whales on the

assumption that the female provides all of her calf's energy needs up to age T_C. They calculated the mean amount of energy expended each day by the calf during this period for maintenance and growth, and then divided this by the average structural mass of the calf x 0.5 (on the assumption that the body condition of both mother and calf was equal to ρ). Similar calculations can be performed for other species, provided a value for σ_G (the energetic cost per unit structural mass) is available.

A DEB model for NE Atlantic harbour porpoise

Suggested parameter values

In this section we describe how values for the individual parameter values of a DEB model for harbour porpoises were selected.

Gestation period (T_P) Lockyer (2003) reviewed estimates of T_P from a number of harbour porpoise populations in the North Atlantic and concluded that it was 10-11 months. We initially used a value of 305 days (approximately ten months) but explored the implications of higher values.

Lactation period/age at weaning (T_L) Lockyer (2003) concluded that the duration of lactation for harbour porpoise was "probably at least eight months", whereas Gaskin (1984) suggest that "it is probably complete within eight months". We chose a value of 250 days (i.e. slightly longer than eight months) but examined the consequences of using higher values.

Structural length and structural mass Table 2 and 3 in Lockyer (2003) provides a mean value of 160 cm for L_∞ in female harbour porpoise from the North Sea, and a length at birth (L_0) of 65-75 cm, we chose the mid-point of that range. None of the published growth curves reported for harbour porpoise (Read and Tolley, 1997; Lockyer et al., 2003; Richardson et al., 2003) replicate these values well: they all predict a lower value for L_∞ and a much higher value for L_0. We, therefore, chose to model length at age using a von Bertalanffy growth curve of the form:

$$L_t = L_\infty - (L_\infty - L_0).e^{-kt}$$

with the growth rate (k) set to 0.0018 cm/day. The resulting curve matches the values in Lockyer's tables, and conforms to her observation that "individuals in most populations have reached their near-asymptotic size by eight years of age" and that a 10-month-old calf brought into captivity measured 115 cm.

Growth in foetal length was assumed to be linear, so that the foetus grows at a constant rate from length 0 cm at conception to L_0 at the end of the gestation period. The structural mass of the foetus was calculated using the relationship $W = 0.00005L^{2.72}$ from Lockyer and Kinze (2003). Estimates of structural mass (S_α) for post-natal animals were based on the relationship:

$$W = 0.000081L_\alpha^{2.67}$$

reported by Lockyer and Kinze (2003). However, W includes the mass of reserve tissue. Based on values in Table 2 of Lockyer (2007) it appears that the average blubber weight for the animals used to estimate this relationship was approximately 27% of total body weight. We therefore used the relationship:

$$S_\alpha = (1\text{-}0.27)*0.000081L_\alpha^{2.67} = 0.000059L_t^{2.6}$$

to estimate structural mass at age.

Field metabolic maintenance scalar (σ_M) The average daily intake of a captive harbour porpoise studied by Kastelein et al. (2018) was 18 MJ, although it was regularly >20 MJ (see Fig. 1f in Kastelein et al. (2018)). Its weight fluctuated between 35 and 42 kg. Assuming these fluctuations are caused by variations in the mass of reserves (see below) and that its core mass remained constant, these values suggest that σ_M for this animal was between 4.5 and 5.1. Given that free-ranging animals are likely to be more active than captive animals, we chose to use a value of 5.5. Hin et al. (2019) concluded that their results were not sensitive to the value used for this parameter and we did not investigate the effects of alternative values.

Energetic cost per unit structural mass (σ_G) We calculated growth efficiency using the same approach as Hin et al. (2019) and an energy density for harbour porpoise foetal tissue of 6.5 MJ/kg (the mean of the values for newborn harp and grey seal pups reported by Worthy and Lavigne (1987)). We considered this to be a more appropriate value than the energy density of fin whale foetal tissue used by Gallagher et al. (2018) for this purpose. This produced a value of 25 MJ/kg for σ_G.

Relative cost of maintaining reserves (Θ_F) We were unable to find any published data that would allow a value specific to harbour porpoises to be calculated for this parameter. We, therefore, suggest using the value of 0.2 assumed by Hin et al. (2019).

Reserve thresholds (ρ, ρ_s) Lockyer (2003) and Kastelein et al. (2018) documented marked seasonal variations in the body weight and blubber thickness of captive harbour porpoises that were closely correlated with changes in water temperature, suggesting that the changes were related more to the thermoregulatory function of blubber than its role as an energy store. Lockyer (2007) documented even larger seasonal variations in the mass of by-caught and stranded animals from the North Sea with the same general pattern as that documented in captive animals. These observations suggest that target body condition and starvation body condition threshold vary over time (i.e. we need to replace constant values with time varying ones), with a maximum value between 1 December and 28 February, and a minimum value on 1 July, which is maintained until around mid-September. Target body condition on 1 July was set at 0.24 based on the lower 95% confidence limit for the proportion of blubber in immature female carcasses reported by McLellan et al. (2002), and this was retained until 15 September. We used the upper 95% confidence limit to set a maximum value for ρ of 0.35.

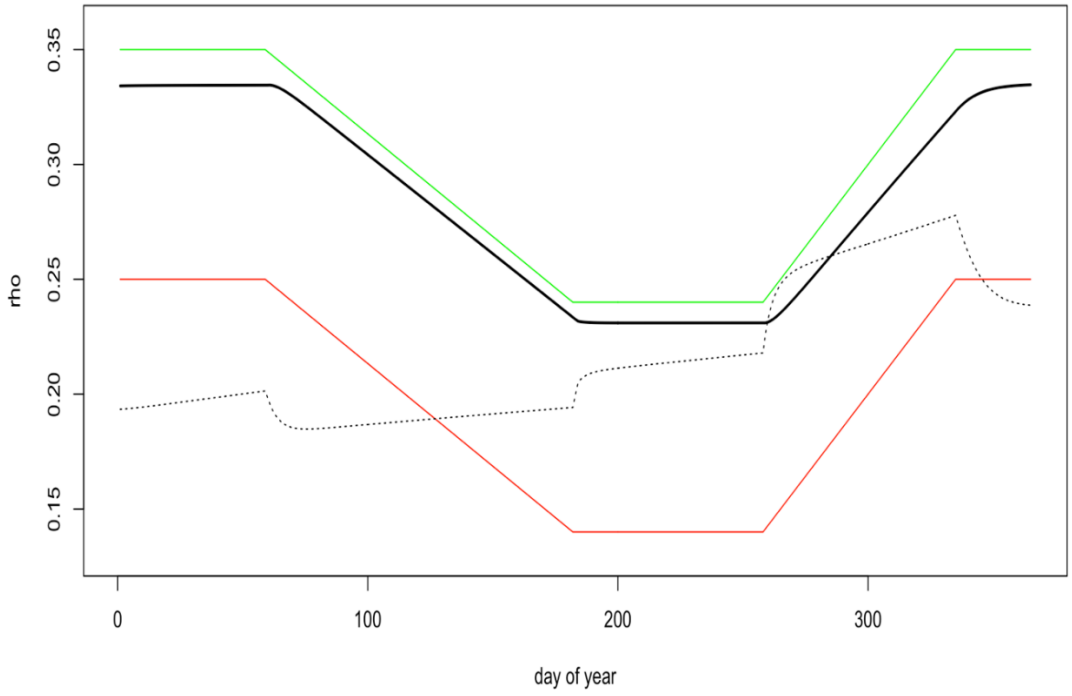

Figure 6: Predicted changes in body condition (rho = ρ) of a two year-old female harbour porpoise who is resting (i.e. neither pregnant nor lactating) – shown by the solid black line – and her daily energy assimilation (dotted black line). Target body condition is indicated by the green line and the starvation body condition threshold is indicated by the red line.

Because the blubber component of an individual's energy reserves plays an important role in thermoregulation, we assumed that ρ_s tracked ρ, with a minimum value of 0.14 between 1 July and 15 September. The latter value was calculated from data in Table 1 of Read (1990), who measured the length and blubber mass of

220 harbour porpoises that were accidentally caught in fishing gear between July and September. Read (1990) presents mean and standard deviation values for seven life history stages. We estimated the mean lean mass of the individuals in each stage using Equation 2 and used this and the 1% quantile for blubber mass to calculate a minimum value for body condition.

Figure 6 shows the changes in ρ and ρ_s over the course of a year, and the predicted changes in daily energy assimilation and body condition for a 2-year-old female that is 'resting' (i.e. neither pregnant nor lactating).

This pattern of change in target body condition resulted in a predicted annual cycle of total body weight for adult animals (Figure 7) that broadly matched observed variations in both captive and wild animals.

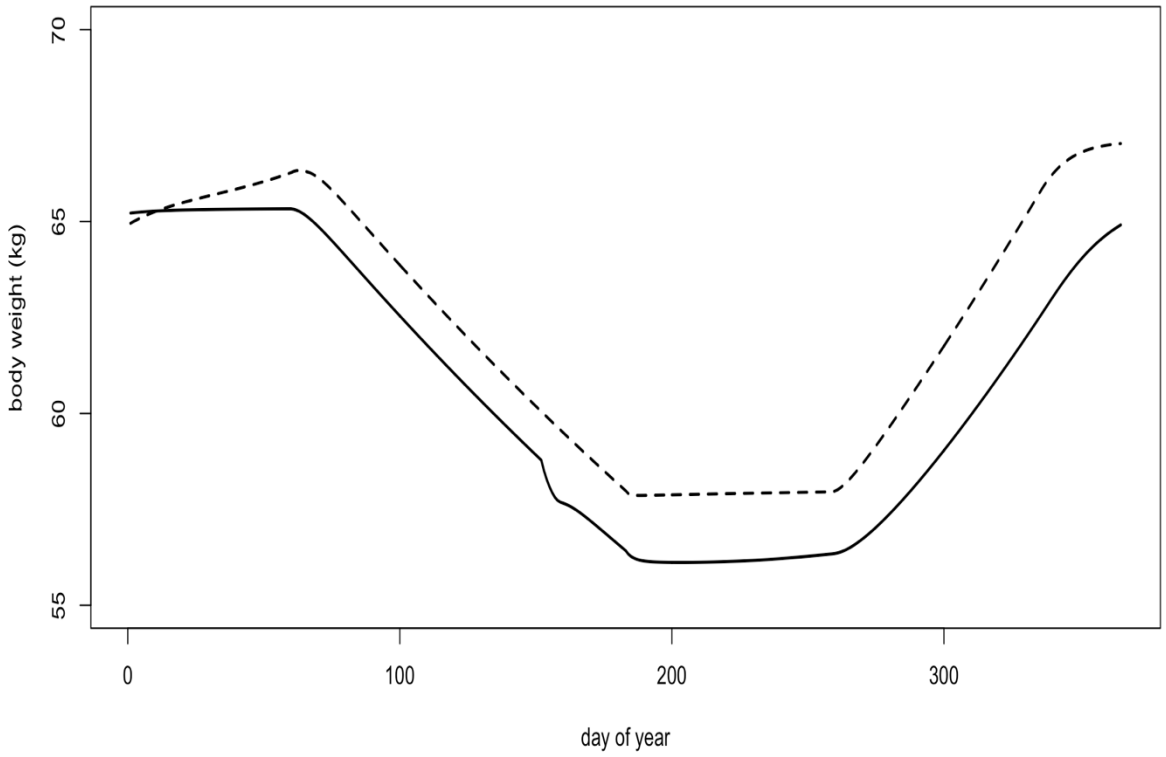

Figure 7: Predicted changes in the total body weight of a mature female harbour porpoise based on the seasonal variations in target body condition shown in Figure 6. The solid line shows the variation in weight when the female is initially pregnant and then lactating. The dotted line shows the same variation when the female is resting (i.e. neither pregnant nor lactating).

Catabolic and anabolic efficiency of reserve conversion (ε^-, ε^+) Because of the large variations in ρ that are predicted to occur over the course of a year, we need two different sets of values for ε and ε^+

$\varepsilon_{\uparrow}^{+}$ and $\varepsilon_{\uparrow}^{-}$ for the period when the target level is increasing over time or it is at its maximum value (i.e. from 1 July to 28 February in the following year) and $\varepsilon_{\downarrow}^{+}$ and $\varepsilon_{\downarrow}^{-}$ for the period when ρ is decreasing (1 March to 30 June).

During the period when ρ is increasing, we assume that animals will catabolize both blubber and lean tissue (as observed in fasting seal pups) and we use a value for $\varepsilon_{\uparrow}$- derived from Kastelein et al. (2019). They observed that near-fasting captive porpoises lost 3.3% of their body weight per day to cover the costs of maintenance. This is similar to the daily weight loss shown by two harbour porpoises immediately after they were brought into captivity, when they did not feed (Lockyer et al. 2003a). The highest recorded daily energy intake of one of the animals studied by Kastelein et al. (2019), which weighed 40 kg, was 26 MJ, suggesting that $\varepsilon_{\uparrow}$- $\simeq$ 20 MJ.kg^{-1} (26/(40*0.033)). If energy assimilation exceeds energy requirements during this period, we assume that individuals will use the energy surplus to build lipid-based reserves, and we use the value $\varepsilon_{\downarrow}^{+}$ = 55 MJ.kg^{-1} from the Hin et al. (2019) pilot whale model.

During the period when ρ is decreasing, we assume that animals whose assimilation is less than their total energy requirements will catabolize lipid ($\varepsilon_{\downarrow}^{-}$ = MJ.kg^{-1}) (Hin et al., 2019) to hasten the reduction in reserve mass, and they will use any surplus energy to build a mixture of blubber and lean tissue ($\varepsilon_{\downarrow}^{+}$ = 20*1.4 = 28 MJ.kg^{-1}).

Efficiency of conversion of mother's reserves to calf tissue, (σ_L) In the absence of any direct measurements of the relevant efficiencies for harbour porpoise, we suggest using the value of 0.86 that was used by Hin et al. (2019).

Steepness of assimilation response (η) We were unable to find any data in the literature that could be used to set a feasible range for this parameter, and we explore the implications of values between 15 and 20.

Effect of age on resource foraging efficiency (γ, T_R) Gaskin (1984) concluded that harbour porpoise calves are capable of taking solid food as early as eight weeks after birth, and they report that Møhl-Hansen (1954) "concluded that they were taking much solid food by five months of age". Learmonth et al. (2014) recorded only solid food in the stomachs of stranded and by-caught calves (animals <110 cm long) collected between January and May (i.e. 6 to 11 months after they had been born). We therefore set T_R at 150 days (≈ 5 months) and γ = 4, implying 100% foraging efficiency by about 18 months of age, but explored the implications of larger and smaller values.

Starvation-induced mortality rate (μ_S) In the absence of any empirical data on this parameter, we explored the effects of a range of values centred on the value of 0.2 used by Hin et al. (2019).

Pregnancy threshold ($F_{neonate}$) The pregnancy threshold determines when females become pregnant for the first time, and also whether or not females can become pregnant while lactating. Lockyer (2003) reported a reproductive interval of 1.01-1.57 years for North Atlantic harbour porpoise and Winship (2009) estimated a birth rates of 0.65 and 0.84, depending on the underlying analytical scenario, for North Sea harbour porpoises, based on an extensive review of data. Both of these estimates imply that a proportion of females are simultaneously lactating and pregnant, and $F_{neonate}$ was adjusted to ensure this was predicted by the model.

Effect of calf age on milk assimilation (ξ_C, T_N) There is no empirical data on when lactating females begin reducing the amount of milk they provide to their calves. Gallagher et al. (2018) assumed this occurs at day 91 of lactation, on the basis of the observations of the start of independent feeding reported above, with a linear decrease from that time onward (i.e. $\xi_C \approx 0.5$). We used these as starting values for our simulations but considered other values.

Effect of female body condition on milk assimilation (ξ_M) Given the relatively short life expectancy of harbour porpoises (compared to other cetaceans) and their high potential reproductive rate, we assumed that lactating females would continue to supply milk to their calves at the normal rate even when their body condition was reduced. We therefore set ξ_M to 0.5, but we explored the implications of using other values.

Lactation scalar (Φ_L) We calculated Φ_L using the same approach as Hin et al. (2019) and arrived at a value of 4.6. This is higher than the value of 2.7 they calculated, probably because the relative costs of maintenance for harbour porpoises are higher than for pilot whales.

A summary of the baseline parameter values for harbour porpoise are presented in Table 2**.**

Table 2

Suggested parameter values for harbour porpoise.

Symbol	Units	Value	Definition	Source
T_P	days	305-335	Gestation period	Lockyer (2003)
T_L	days	250-280	Age at weaning	Gaskin (1984), Lockyer (2003)
L_0	cm	70	Length at birth	Lockyer (2003)
L_∞	cm	160	Asymptotic length	Lockyer (2003)
k	cm.day^{-1}	0.0018	Von Bertalanffy growth coefficient	
ω_1	kg·cm^{-1}	5.9x10^{-5}	Structural mass-length scaling constant	Derived from Lockyer and Kinze (2003)
ω_2	–	2.67	Structural mass-length scaling exponent	Lockyer and Kinze (2003)
K	MJ·kg^{-1}.day^{-1}	0.294	Mass-specific Resting Metabolic Rate	Kleiber (1975)
σ_M	-	5.5	Field metabolic maintenance scalar	Derived from data in Kastelein et al. (2018)
σ_G	MJ·kg^{-1}	25	Energetic cost per unit structural mass	Calculated using the approach of Hin et al. (2019)
θ_F	–	0.2	Relative cost of maintaining reserves	Hin et al. (2019)
ρ	–	0.24/0.35	Target body condition. Summer/winter	Derived from data in Lockyer (2007), McLellan et al. (2002)
ρ_S	–	0.14/0.25	Starvation body condition threshold	Derived from data in Read (1990)
$\varepsilon_{\uparrow -}$	MJ·kg^{-1}	20	Catabolic efficiency of reserves conversion when ρ is increasing or constant	Derived from data in Kastelein et al. (2019)
$\varepsilon_{\uparrow +}$	MJ·kg^{-1}	55	Anabolic efficiency of reserve conversion when ρ is increasing or constant	Hin et al. (2019)
$\varepsilon_{\downarrow -}$	MJ·kg^{-1}	35	Catabolic efficiency of reserves conversion when ρ is decreasing	Hin et al. (2019)

$\varepsilon_{\downarrow+}$	MJ·kg^{-1}	28	Anabolic efficiency of reserves conversion when ρ is decreasing	1.4x $\varepsilon_{\uparrow-}$, Hin et al. (2019)
σ_L	–	0.86	Efficiency of conversion of mother's reserves to calf tissue	Hin et al. (2019), based on data in Lockyer (2003)
η	–	15-20	Steepness of assimilation response	None. We explore the implications of values between 15 and 20
γ	–	4	Shape parameter for effect of age on resource foraging efficiency	
T_R	days	130-150	Age at which calf's resource foraging efficiency is 50%	Gaskin (1984)
μ_s	-	0.2	Starvation mortality scalar	Hin et al. (2019)
T_N	days	91-120	Calf age at which female begins to reduce milk supply	Gallagher et al. (2018)
ξ_C	–	0.5	Non-linearity in milk assimilation-calf age relation	Gallagher et al. (2018)
ξ_M	–	1-3	Non-linearity in female body condition-milk provisioning relation	Hin et al. (2019)
φ_L	-	3.55	Lactation scalar	Calculated using the approach of Hin et al. (2019)

Other components of the DEB model

Survival and Life Expectancy: Hin et al. (2019) used published information on the age-structure of the Northeast Atlantic long-finned pilot whale population to calculate an age-dependent mortality schedule and a matching cumulative survival curve. An equivalent cumulative survival curve for North Sea harbour porpoise was derived from the age-specific survival rates estimated by Winship (2009) using his Scenario 2. The maximum age was set to 30 years, and the survival of age-classes 25-30 was reduced to 0.3, so that only 1 in 10,000 animals was predicted to survive to this age. The resulting cumulative survival curve is shown in Figure 8.

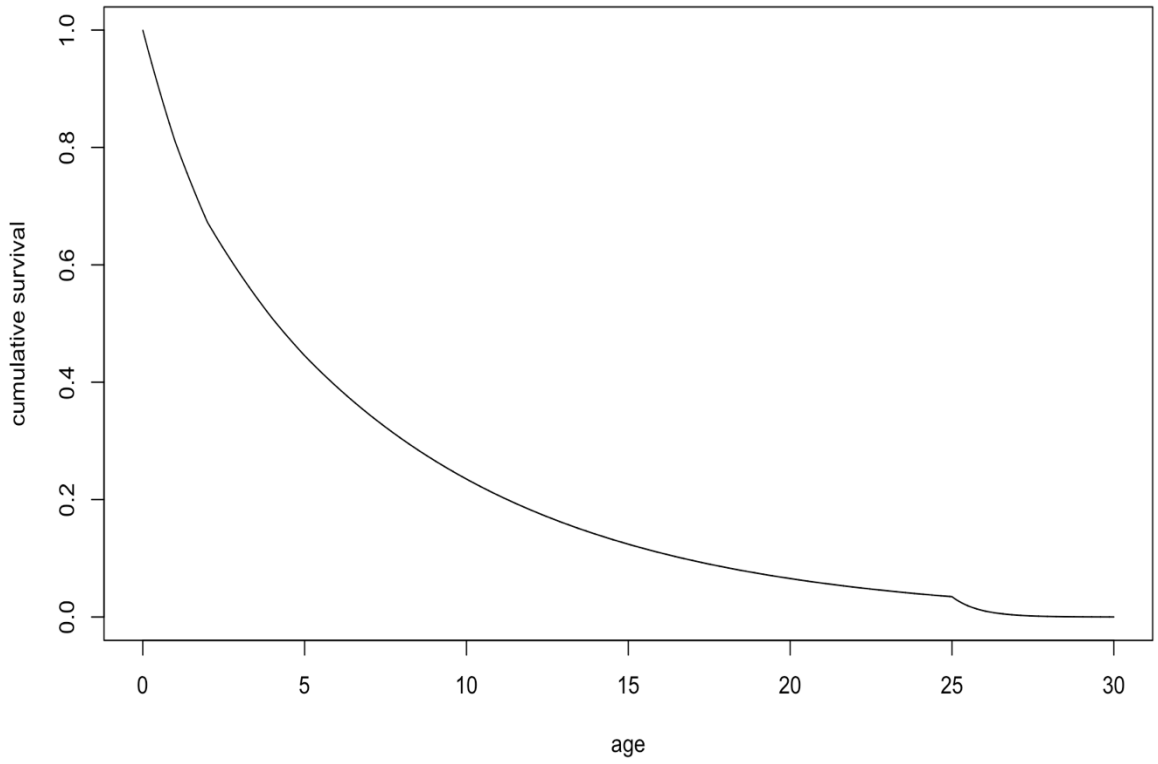

Figure 8: Cumulative survival curve for harbour porpoises in the North Sea based on age-specific survival estimates in Winship (2009).

The life expectancy of each simulated individual was set by drawing a random number between 0 and 1. Death was presumed to occur at the age when the cumulative survival probability shown in Figure 8 fell below this value. This process ensures that the simulated individuals represent a random sample of all possible female life histories. As a result, their mean reproductive success can be used as an estimate of the population growth rate (λ).

In addition to background mortality, simulated females and calves were assumed to suffer from an increased risk of mortality if their relative body condition fell below a pre-defined starvation threshold (ρ_s). Survival on each day that ρ_t was below this threshold was determined by conducting a binomial trial with the probability ϕ_t defined by Equation 1.

Energy expenditure: The daily cost of growth is calculated as the difference in structural mass between consecutive days multiplied by the energy cost per unit of structural growth σ_G = 25 MJ.kg^{-1}.

Daily field metabolic costs (FM_t) are assumed to be a multiple (σ_M) of the animal's maintenance mass to the power 0.75, following Kleiber (1975):

$$FM_t = \sigma_M.K.(S_t + \theta_F F_t)^{0.75}$$

A female is assumed to be capable of becoming pregnant if her reserve mass exceeds $F_{neonate}$. In order to become pregnant, a female must ovulate successfully, this ovum must be fertilised and the resulting embryo must implant successfully. The model assumes that all females older than three years ovulate every year. Implantation can occur if the female's relative body condition is above the threshold for pregnancy on at least one day during a 10-day period starting on 1 August, assuming that most births occur on 1 June and a gestation period of ten months. If the female meets this condition, the model assumes there is that she will become pregnant in that year, based that Murphy et al. (2015) found a 1:1 relationship between age and corpora number for harbour porpoises that stranded in UK waters between 1990 and 2012.

During pregnancy, females must cover the costs of foetal growth and foetal maintenance, unless the foetus dies. Murphy et al. (2015) documented a 19.7% mortality of foetuses in their sample of stranded animals and we incorporated this value in our simulations. The mass of the foetus was included in the female's maintenance mass, so the cost of foetal maintenance is included in her maintenance costs. In addition, females are assumed to transfer additional energy to their foetus at birth so that its body condition is equivalent to the minimum value of ρ_s.

Model properties

Hin et al. (2019) assumed that female pilot whales only become pregnant if their energy reserves are sufficient to cover all the energetic costs of that pregnancy, and provide a buffer against the risk of starvation mortality. Harbour porpoises are too small to accumulate reserves of this magnitude. We, therefore, investigate the sensitivity of the model to various plausible modifications of this threshold.

Figure 9 shows part of the life history of a typical simulated female using a pregnancy threshold that covers 60% of foetal growth costs as well as avoiding the risk of starvation mortality, and the baseline parameter values listed in Table 2. Young females struggle to raise a calf successfully and the first three calves die from starvation. In the case of the first two calves, the female's body condition is below the threshold for a successful pregnancy at the time ovulation occurs and she therefore fails to give birth to a calf in the next year (i.e. she shows a two-year reproductive cycle). However, she does become pregnant while raising the third calf (even though it dies before weaning) and gives birth in the next year. Subsequently, she produces a calf every year until her eventual death.

The average inter-calf interval for simulated females was 1.35 years, and the average birth rate was 0.72. Both values are within the ranges reported by Lockyer (2003) and Winship (2009), but substantially higher than the birth rate of 0.5 reported by Murphy et al. (2015). In addition, body condition declined with increasing age (as reported by Lockyer, 2003), as the females spent more of their time lactating.

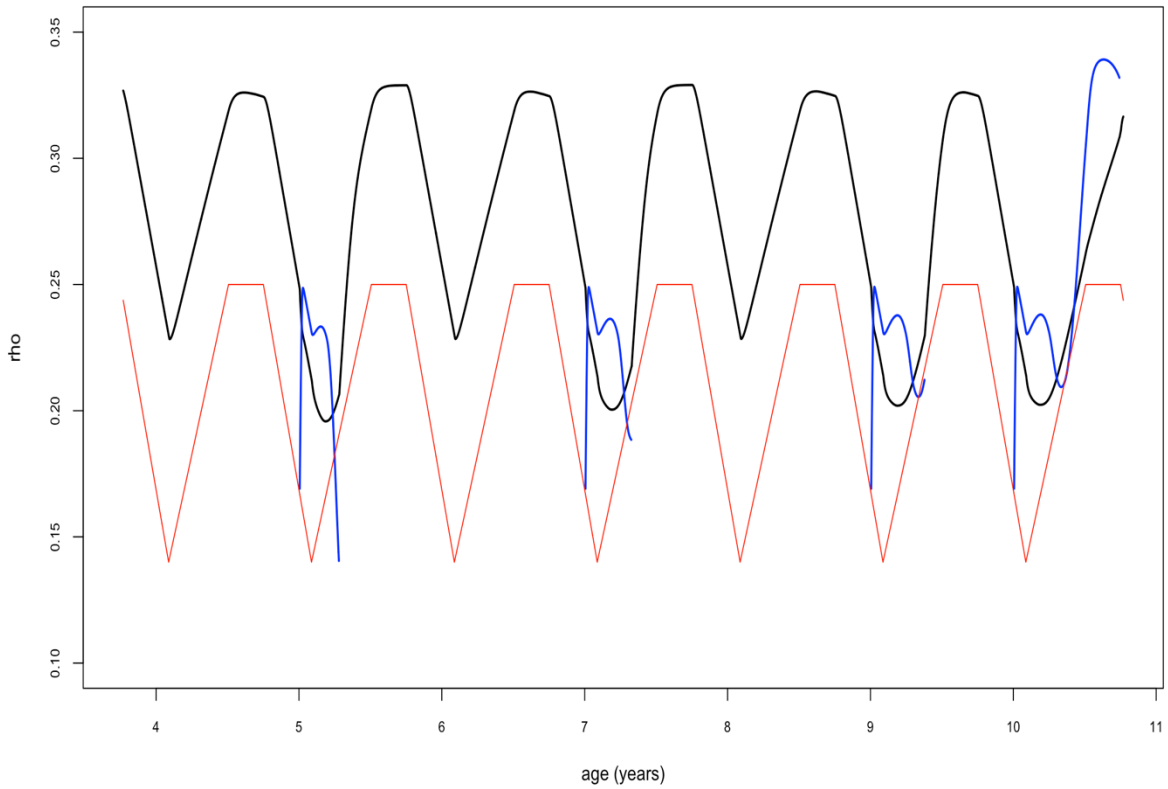

Figure 9: Variations in the body condition (rho = ρ) of a simulated female harbour porpoise (shown in black) and her first four calves (shown in blue). The red line is the starvation body condition threshold for both female and calves. The body condition of the first three calves falls below the starvation threshold soon after the female begins reducing the amount of milk she provides to the calf, and these calves die. The fourth calf is weaned successfully.

We then explored the sensitivity of the model predictions to different values of some of the key model parameters. First, we adjusted R (the resource density) until the mean reproductive success of 5,000 simulated females was close to 1.0, implying that the population of which they are part will be neither increasing nor decreasing (i.e. stationary). We then varied individual parameter values and recorded the effect of mean reproductive success.

Increasing the age at weaning (T_L) to 280 days, the steepness of the assimilation response (η) to 20, and the age at which females being to reduce their milk supply (T_N) to 120 days all resulted in a substantial increase in reproductive success. Since there is empirical evidence to support these alternative values, we incorporated them

into the model and calculated a new value for R that corresponded to a stationary population.

Modifying the gestation period (T_P) to 11 months, rather than ten, had very little effect, as did varying the starvation mortality scalar (μ_s). However, varying the age at which the calf's foraging efficiency is 50% (T_R) had a dramatic effect. If T_R was increased from 150 days to 180 days, all calves died because they were unable to compensate for the reduction in milk supply that occurred from age 120 days onwards. On the other hand, reducing T_R to 130 days resulted in a substantial increase in calf survival (from 0.50 to 0.78), with a consequential effect on reproductive success. This "knife-edge" response demonstrates the potential sensitivity of the model's predictions to parameter mis-specification.

Reducing the parameter ξ_M, which determines how rapidly a female reduces the milk supply if her body condition declines, from two to one resulted in almost all calves dying. Increasing its value to three resulted in an increase in calf survival, but further increases had very little effect. We, therefore, reset ξ_M to three and T_R to 130 days, and calculated a new value for R. The analysis of the effects of disturbance in the next section was carried out using these new baseline values (which are also shown in Table 2).

In order to generate model predictions of birth rate that coincided more closely with Murphy et al.'s (2015) recent observations for harbour porpoises in UK waters, we increased $F_{neonate}$, so that the female was able to cover the entire costs of foetal growth as well as avoiding the risk of starvation mortality. Figure 10 shows the predicted changes in body condition of a 10-year-old female and her two calves over two reproductive cycles using this value.

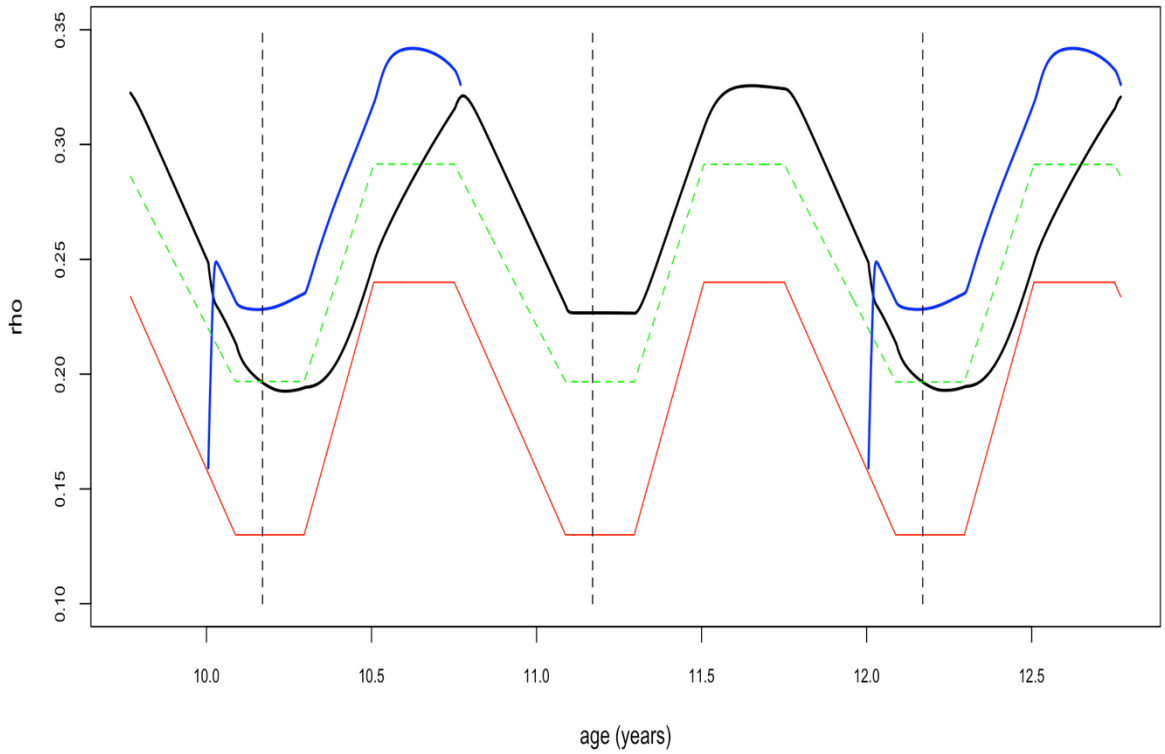

Figure 10: Predicted variations in the body condition (rho = ρ) of a simulated 10-year old female harbour porpoise (shown in black) and her calves (shown in blue) over two reproductive cycles, using the final baseline parameter values. The red line is the starvation body condition threshold and the green line is the pregnancy threshold. The vertical dotted line marks the first day on which the female is able to become pregnant.

They resulted in a calf survival from birth to weaning of 0.76, a mean birth rate of 0.52 and a mean inter-calf interval of 1.95 years. During the first lactation period shown in Figure 10 the females body condition is just below the threshold for pregnancy, and she does not therefore produce a calf in the next year. However, in this year her body condition is well above the threshold and she becomes pregnant again. Although this parameterisation results in a birth rate much closer to that reported by Murphy et al. (2015) the resulting reproductive history appears to be highly risky, with the female's body condition very close to the threshold for starvation mortality for long periods during lactation. If there is any variation in resource density from day to day, as seems very likely, there is a high risk that the female will die from starvation during one of these periods.

We therefore incorporated day-to-day variability in resource density (R) using a beta function (to ensure the resource density was always greater than zero) with mean 0.25 and standard deviation 0.075, which was rescaled to match the required mean value for R. This resulted in predicted variations in the energy intake of sub-adult animals that fell well within the potential range calculated by Booth (2020) based on measured prey capture rates from tagged porpoises and estimates of the energy

density of their potential prey species. As expected, a higher value of R was required for equilibrium ($\lambda = 1$), but the resulting reproductive strategy appears less risky (Figure 11).

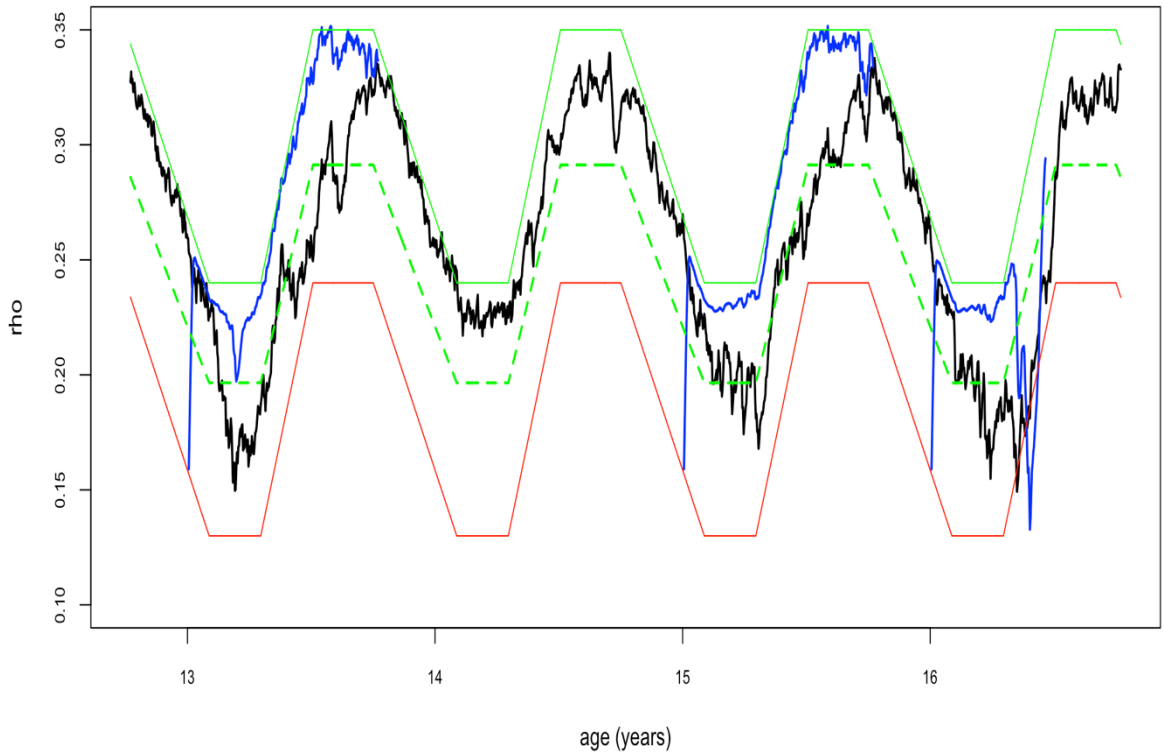

Figure 11: Predicted variations in the body condition (rho = ρ) of a simulated 13-year old female harbour porpoise (shown in black) and her calves (shown in blue) over three reproductive cycles when resource density varies from day to day. The red line is the starvation body condition threshold, the dotted green line is the pregnancy threshold, and the solid green line is the target body condition.

Unfortunately, the stochasticity in R results in lower calf survival (0.68) and, therefore, a higher birth rate (0.61) is required to achieve a mean reproductive output of one. We, therefore, increased $F_{neonate}$, so that the female was able to cover the entire costs of foetal growth and the additional energy supplied to the calf at birth from her energy reserves, while still avoiding the risk of starvation mortality. The resulting model predictions, with and without variation in resource density, are shown in Figures 12 and 13. The birth rate with a constant value for R *was* 0.53. When R was allowed to vary, the birth rate was 0.54.

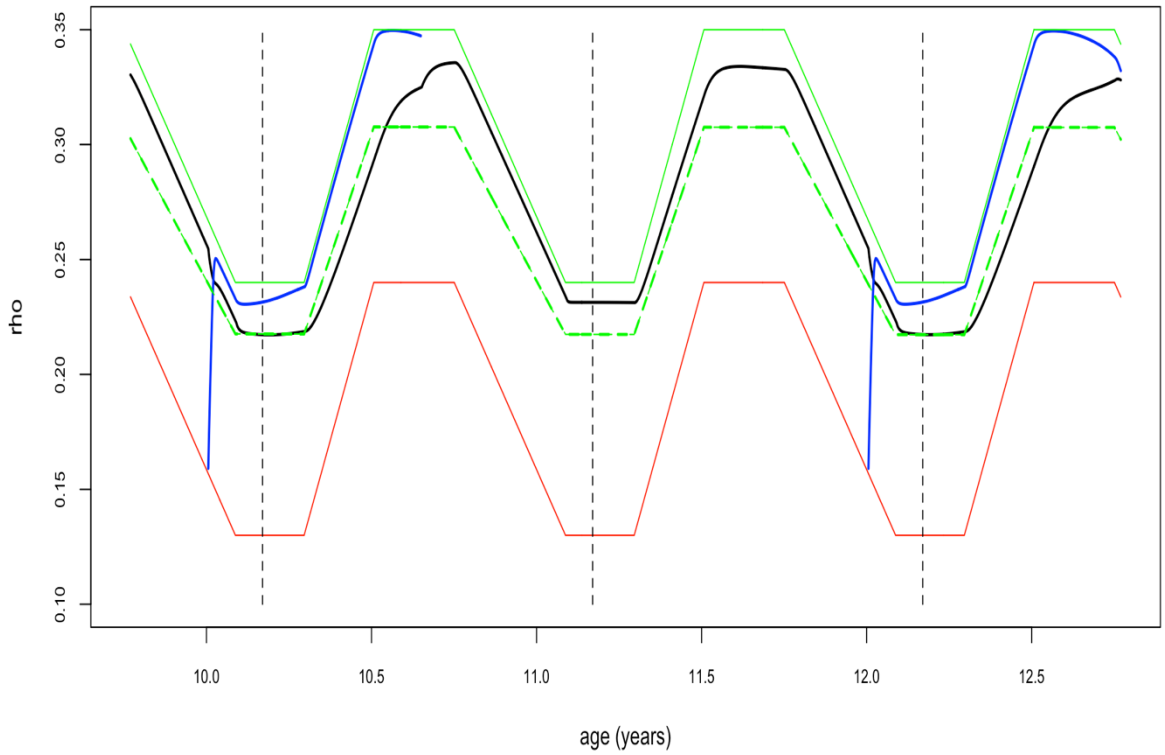

Figure 12: Predicted variations in the body condition (rho = ρ) of a simulated 10-year old female harbour porpoise (shown in black) and her calves (shown in blue) over two reproductive cycles when resource density is constant and the pregnancy threshold is higher than that used in Figures 10 and 11. The red line is the starvation body condition threshold, the dotted green line is the pregnancy threshold, and the solid green line is the target body condition.

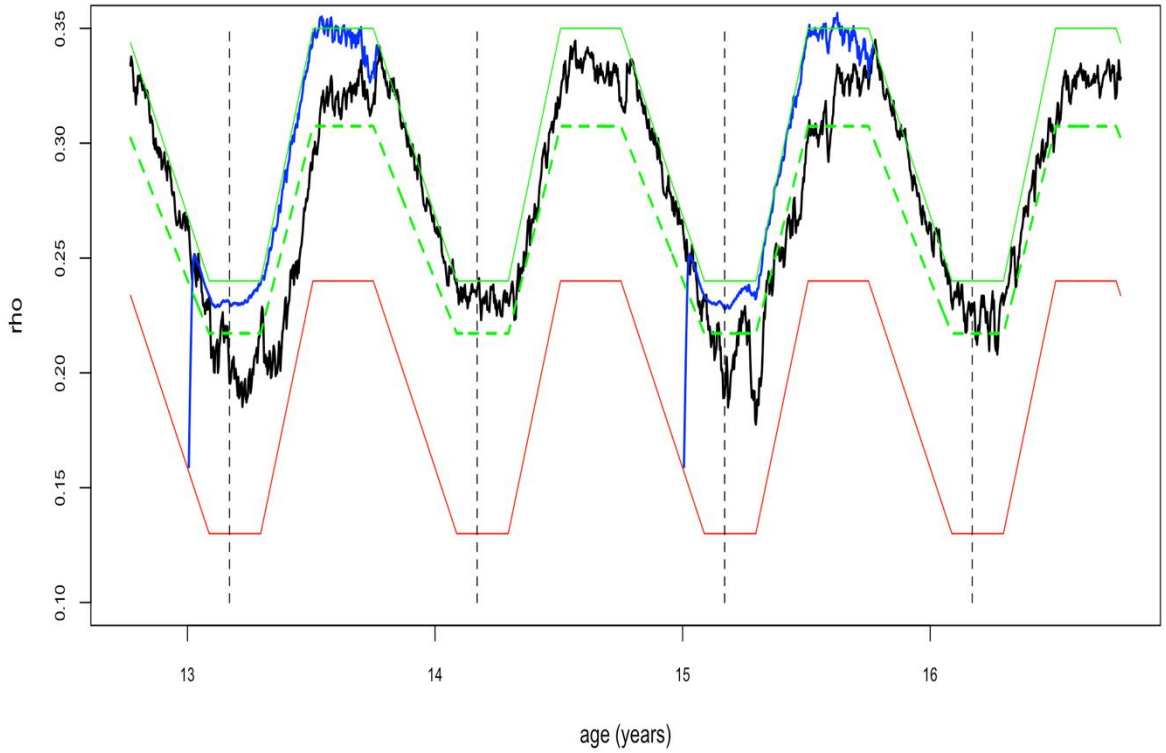

Figure 13: Predicted variations in the body condition (rho = ρ) of a simulated 13-year old female harbour porpoise (shown in black) and her calves (shown in blue) over two reproductive cycles when resource density varies from day to day and the pregnancy threshold is higher than that used in Figures 10 and 11. The red line is the starvation body condition threshold, the dotted green line is the pregnancy threshold, and the solid green line is the target body condition.

The analyses of the potential effects of disturbance on calf survival and birth rate in the next section were carried out using these two values for $F_{neonate}$, both without and with environmental variation.

Predicting the effects of disturbance on harbour porpoise using a DEB model

Introduction

In this section we illustrate how the DEB model can be used to investigate the potential effects of disturbance that causes a reduction in energy intake and subsequent effect on vital rates (individual survival and birth rate). The results we show here depend very much on the specific set of model parameter values that are used and therefore should not be considered as estimates of the potential effects of this kind of disturbance on harbour porpoise populations. Such estimates would require an exhaustive exploration of the feasible parameter space that is beyond the scope of this report.

We divided the harbour porpoise year into four periods:

- **1 June – 31 July:** This covers the time from birth to fertilisation. It is the only period when disturbance can affect birth rate because this is determined only by an individual's age and its body condition relative to the pregnancy threshold at the time of fertilisation.
- **1 August – 30 September:** This covers the time from potential implantation of the embryo to the day on which the female begins to reduce the amount of milk she provides to her calf.
- **1 October – 7 March:** This covers the remainder of the time during which the female is providing milk to the calf.
- **8 March – 31 May:** This covers the post-weaning period up to the calf's first birthday.

We assumed that an individual's energy intake would be reduced by 25% on the day it was disturbed, because this was one of the outcomes of the expert elicitation described in Booth et al. (2019). For a particular disturbance scenario, we selected the required number of days at random from the total number of days in the period. Although we did not test this, it is likely that a more aggregated distribution of disturbance days (i.e. with more consecutive days of disturbance) would result in greater effects on vital rates than those reported here.

The effect of disturbance on calf survival was estimated by determining the proportion of 500 simulated calves (1,000 when R was allowed to vary) that died of starvation-related mortality during the period. According to the model specification, the only time that disturbance can affect birth rate is during the period 1 June – 30 July. We calculated this effect by comparing the proportion of simulated females that became pregnant during this period when there was disturbance, and when there was none.

Results

8 March – 31 May (post-weaning to age one)

In all our simulations, the weaned calf starts this period in good body condition because the target body condition is high (ρ_t = 0.343). Their target body condition decreases over the subsequent three months, so the calf does not require a particularly high energy acquisition rate to meet this target. As a result, it is easily able to compensate for the small changes in body condition that result from disturbance and even 50 days of disturbance did not result in the body condition of

any simulated calf falling below the starvation body condition threshold. Essentially, these results imply that disturbance during this period is unlikely to affect survival.

1 June – 31 July (birth to fertilisation)

The effects of disturbance during this period varied markedly among the four scenarios. With the lower threshold for pregnancy and constant resource density (dotted black line in Figure 14) calf mortality increased sharply when there was 10-20 days of disturbance (i.e. 10-20 days upon which the female's energy intake was reduced by 25% each day). However, mortality increased more slowly with increasing days of disturbance when variation in resource density was introduced into the model (solid black line in Figure 14). With a higher threshold for pregnancy (blue lines in Figure 14), the effects of disturbance on calf mortality were substantially reduced, with no effect being observed until disturbance occurred on 30 or more days in some scenarios.

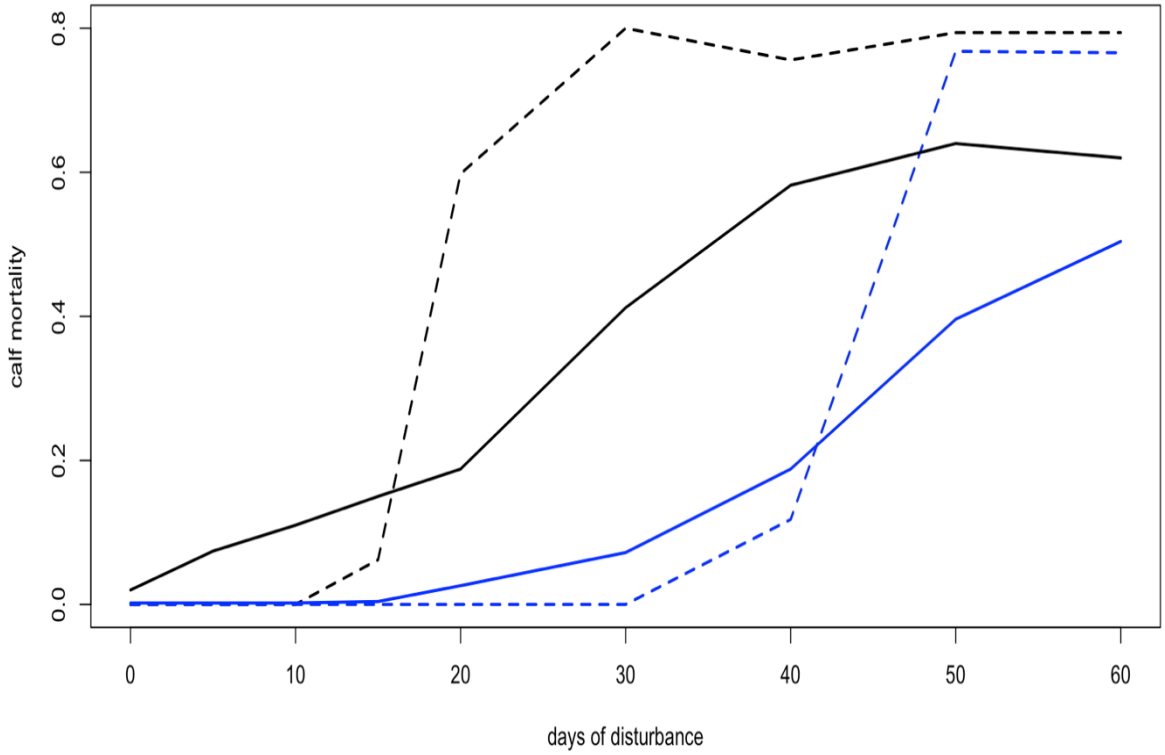

Figure 14: Predicted effect of increasing number of days of disturbance during the period 1 June – 31 July on calf mortality in simulations with (solid lines) and without (dotted lines) day-to-day variation in resource density. Black lines represent scenarios with a relatively low threshold for pregnancy, and blue lines are for scenarios with a higher threshold.

Similar changes were observed in the effect of disturbance on birth rate. However, the difference between scenarios in which resource density was allowed to vary from day to day (solid lines in Figure 15) and those in which it remained constant (dotted

lines in Figure 15) was much more marked. As we will discuss later, the apparent dramatic effect of disturbance on birth rate in a constant environment is almost certainly an artefact of the equilibrium conditions associated with the specific combination of age-specific survival rates used in these simulations.

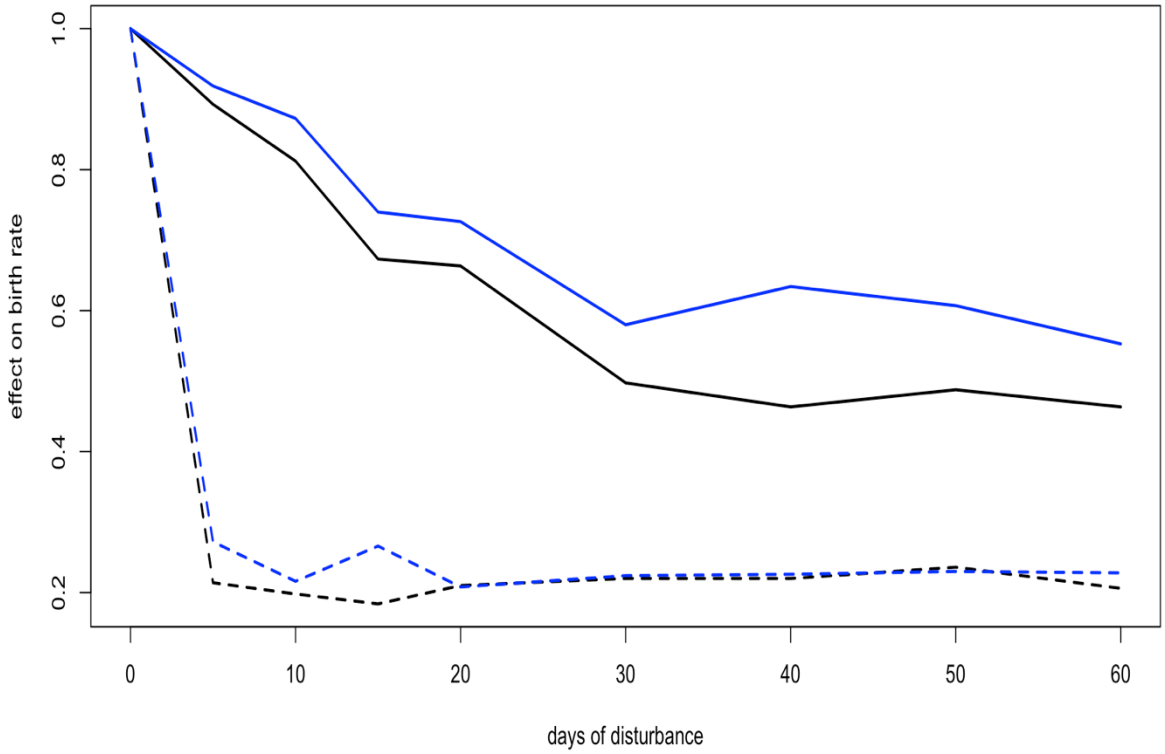

Figure 15: Predicted effect of increasing number of days of disturbance during the period 1 June – 31 July on birth rate in simulations with (solid lines) and without (dotted lines) day-to-day variation in resource density. Black lines represent scenarios with a relatively low threshold for pregnancy, and blue lines are for scenarios with a higher threshold.

1 August – 30 September (embryo implantation to reduction in milk provision)

The predicted effect of disturbance during this period was similar to the previous period (Figure 16), although the sharp increase in mortality in scenarios with constant resource density occurred at slightly lower levels of disturbance and the rate of increase was even greater.

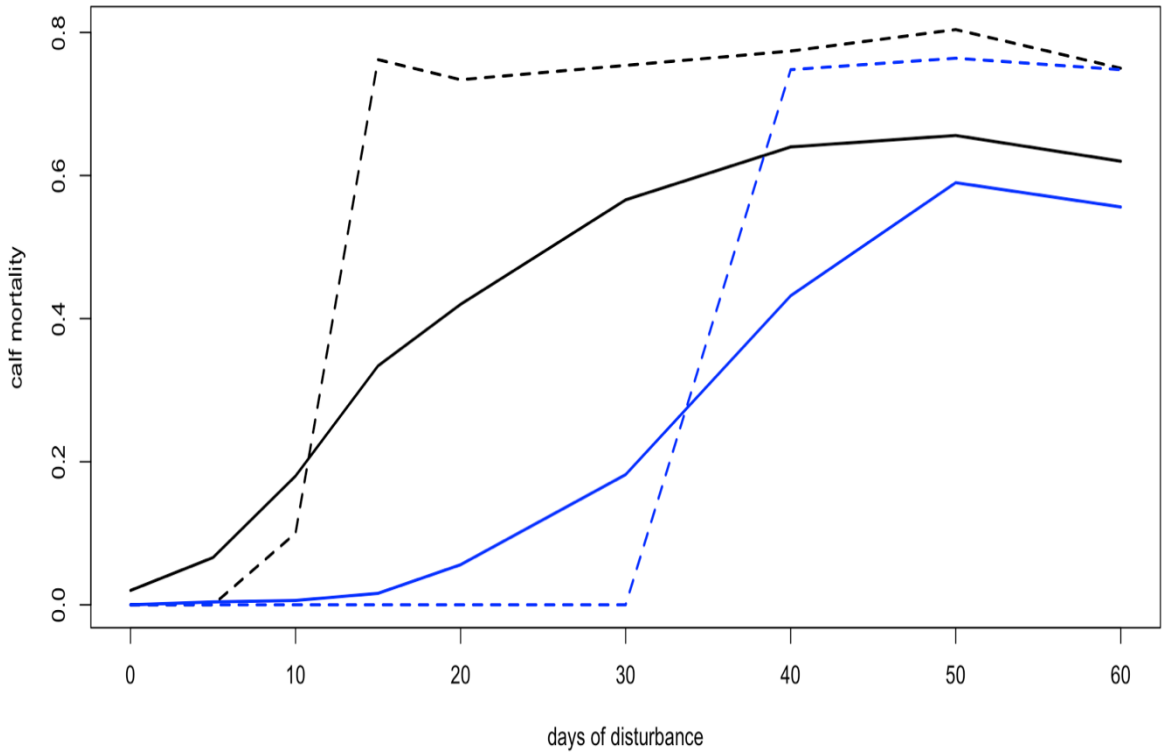

Figure 16: Predicted effect of increasing number of days of disturbance during the period 1 August – 30 September on calf mortality in simulations with (solid lines) and without (dotted lines) day-to-day variation in resource density. Black lines represent scenarios with a relatively low threshold for pregnancy, and blue lines are for scenarios with a higher threshold.

1 October – 7 March (remainder of lactation period)

During this period, the calf is increasingly able to provide most of the energy it requires for maintenance and growth from its own foraging efforts, and disturbance has less effect on calf mortality than it did during the period when the calf is entirely dependent on its mother (Figure 17). In fact, disturbance was predicted to have almost no effect in scenarios where resource density varied from day to day (blue lines in Figure 17).

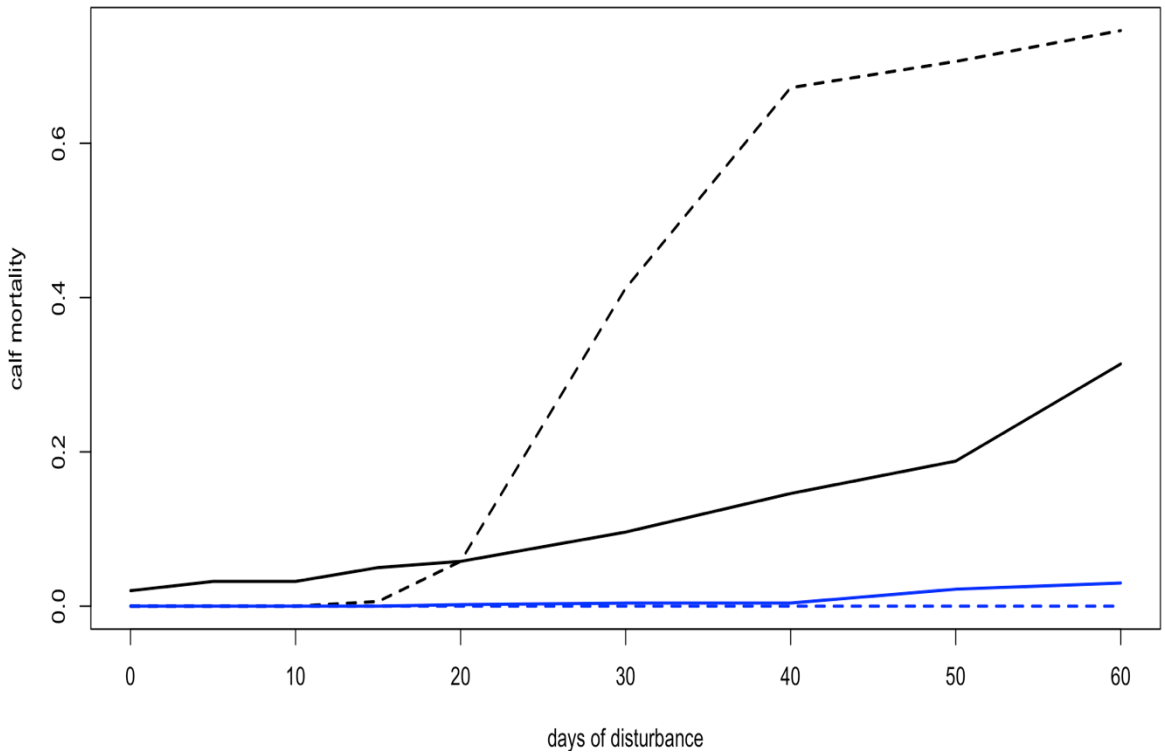

Figure 17: Predicted effect of increasing number of days of disturbance during the period 1 October – 7 March on calf mortality in simulations with (solid lines) and without (dotted lines) day-to-day variation in resource density. Black lines represent scenarios with a relatively low threshold for pregnancy, and blue lines are for scenarios with a higher threshold.

Discussion

The results presented here are a consequence of the specific implementation of the DEB model described in the previous section. We only varied one parameter of the model ($F_{neonate}$, the threshold for the onset of pregnancy), but this had a large effect on the predicted effect of disturbance on calf survival. Simulations conducted with other parameters of the model but not presented here indicate a similar sensitivity to variation in T_R (the age at which the calf feeding efficiency is 50%).

We chose parameter values that effectively maximized mean reproductive output for a particular resource density. However, this resulted in risky reproductive strategies that were potentially vulnerable to the effects of a temporary reduction in energy intake. Pirotta et al. (in Review) identified a similar issue when they used stochastic dynamic programming to identify the reproductive strategy that optimised fitness for the Hin et al. (2019) DEB model. They resolved that issue by optimising the model for a variable environment. We observed the same effect when we incorporated variation in resource density into the harbour porpoise model: the effects of disturbance on vital rates were substantially reduced.

The extreme effect on disturbance on birth rate shown in Figure 15 is almost certainly an artefact of the specific age-specific survival values used in these simulations. The birth rate at equilibrium (i.e. when mean reproductive output = 1) with these values is slightly higher than 0.5. To achieve this, females must alternate between a two-year and a one-year reproductive cycle. In these simulations, the body condition of lactating females is very close to the threshold for pregnancy at around the time of implantation (see Figure 12, where the black line indicating female body condition and the green dotted line indicating the pregnancy threshold overlap during lactation). Very small changes in energy intake can flip the female out of a one-year cycle. This risk is much reduced by including variation in resource density and could be further reduced by small changes in age-specific survival. For example, when we repeated the simulations using the age-specific survival rates recommended by Sinclair et al. (2020), where annual adult survival is set to 0.925 rather than 0.88, all females were predicted to adopt a 2-year reproductive cycle and very high levels of disturbance (50 days or more) in the period 1 June – 31 July were required to have any effect on birth rate.

These analyses demonstrate the sensitivity of the DEB model predictions to uncertainty in its parameter values. However, investigating the implications of this uncertainty is a non-trivial exercise. It is not a matter of simply sampling from a statistical distribution or plausible range for each parameter and documenting the consequences. Each parameter combination results in a unique set of values of reproductive output depending on the resource density (R). Reproductive output affects susceptibility to disturbance (populations with high mean reproductive output are less sensitive to disturbance than those with low outputs). It is, therefore, necessary to find the R value associated with each combination of parameter values that results in a stable population (mean reproductive output ≈ 1) in order to make valid comparisons between model implementations. Unfortunately, there is no simple formula for calculating this value; it has to be derived iteratively. In addition, it is not obvious how to choose an appropriate range or statistical distribution for many of the parameters.

There are, however, some clear messages. If the formulation of the model is correct, and it seems to reproduce many of the observed characteristics of Northwest Atlantic populations, nursing female harbour porpoises are particularly susceptible to disturbance during the period from the time the calf is born until it is able to acquire at least some food independently. Outside this period, the effects of disturbance are relatively modest. Some of the effects of disturbance during early lactation may carry over into the second half of lactation, but animals will probably have been able to

compensate for all of the effects of disturbance in one year by the beginning of the next breeding season. This is one of the fundamental assumptions of the iPCoD model.

Integrating DEB model outputs into iPCoD

The DEB model for pilot whales developed by Hin et al. (2019) can be parameterised for UK and Northeast Atlantic populations of the five marine mammal species included in the Interim PCoD framework using values obtained from the literature, as presented in Section 3. However, some of the parameters which potentially have a large effect on susceptibility to disturbance cannot be measured directly and appropriate values have to be chosen subjectively. Further work is required to identify parameter combinations that result in more robust reproductive strategies.

However, accounting for uncertainty in the model parameters will be challenging conceptually, because we need a more formal approach to identifying suitable measures of uncertainty for the subjectively determined parameters, and technically, because a unique value of the equilibrium resource density has to be determined for each combination of parameter values. Nevertheless, we believe this could be achieved relatively efficiently by a 1-2 day workshop involving UK-based experts who should be able to agree on plausible ranges for the relevant model parameters. The efficiency of the code implementing the DEB model can certainly be improved and this would allow model predictions that accounted for plausible levels of uncertainty to be generated.

Once the issues relating to uncertainty have been addressed, relationships of the kind shown in Figures 14-17 can be incorporated into the iPCoD code without major structural changes, because the code models day-by-day exposure to disturbance for a large number of simulated individuals. Each exposure history can be combined with those relationships to predict the effects of exposure on disturbance on that simulated individual. However, the movement model used to simulate exposure histories is simplistic. It assumes that all individuals in a population are equally likely to be exposed to disturbance from a particular activity, or that only the members of a local population are likely to be exposed. The real-world situation is likely to be somewhere between these two extremes, and a more detailed movement model is required to generate more realistic exposure histories.

Recent developments in the use of DEB models to investigate the effect of multiple chemical stressors on individual health (the DEBtox approach) could provide a framework for implementing the model structure proposed by the National

Academies Committee on the Assessment of the Cumulative Effects of Anthropogenic Stressors on Marine Mammals (Figure 5.3 in National Academies of Sciences Engineering and Medicine, 2017). However, these particular DEB models have, to date, only been developed for laboratory populations, and it will be some time before models that can be applied to free-ranging populations are available.

Conclusions

This work has demonstrated that the DEB model for pilot whales developed by Hin et al. (2019) can be parameterised for each of the five key UK marine mammal species, using a combination of values derived from the literature and those estimated by subjective judgement. The sensitivity testing and scenario demonstrations have shown that some of the parameters which potentially have a large effect on susceptibility to disturbance cannot be measured directly and therefore have to be chosen subjectively. This should be a key consideration if DEB models are used to predict the effects of disturbance.

Recommendations

The following tasks are required in order to fully develop DEB models for the five key UK marine mammal species, and to incorporate them into the iPCoD framework:

- Production of DEB models of the remaining species: bottlenose dolphins, minke whales, grey seals and harbour seals using the parameter values proposed in Appendices 1-4.
- Workshop(s) to agree on plausible ranges for DEB model parameters for each species.
- Incorporation of results from explicit models of movement into iPCoD to generate more realistic exposure histories.
- Modification of the iPCoD framework code to incorporate DEB models (if required).

Appendix 1

Suggested parameter values for DEB models for bottlenose dolphins

The suggested parameter values for bottlenose dolphins are shown in Table 3, and details of how these parameters were derived are outlined below. These values should serve as a useful starting point for model development, but they will probably need to be refined as modelling progresses. The rationale behind the choice of these values is given in Appendix 1. Note that many of the values relating to body condition are derived from the long-term study of bottlenose dolphins in Sarasota Bay, where water temperatures (especially in summer) are much higher than those likely to be experienced by UK animals and where dolphins are, on average, smaller than those found in the UK. It would be valuable to have equivalent data for a UK population, but this would be extremely challenging because it requires regular live-capture and handling of individuals.

Table 3

Suggested parameter values for bottlenose dolphins.

Symbol	Units	Value	Definition	Source
T_P	days	365	Gestation period	Perrin and Reilly (1984)
T_L	days	550-600	Age at weaning	Kastelein et al. (2002)
L_0	cm	165	Length at birth	Cheney et al. (2018)
L_∞	cm	333	Maximum length	Cheney et al. (2018)
ω_1	$kg \cdot cm^{-1}$	$10^{-5.03}$	Structural mass-length scaling constant	Emaciated animals, Hart et al. (2013)
ω_2	–	3.01	Structural mass-length scaling exponent	Emaciated animals, Hart et al. (2013)
K	$MJ \cdot kg^{-1}.day^{-1}$	0.294	Mass-specific Resting Metabolic Rate	Kleiber (1975)
σ_M	-	4.5 – 6.0	Field metabolic maintenance scalar	Field measurements from Bejarano et al. (2017)
σ_G	$MJ \cdot kg^{-1}$	30	Energetic cost per unit structural mass	Hin et al. (2019)
θ_F	–	0.2	Relative cost of maintaining reserves	Hin et al. (2019)
ρ	–	0.35	Target body condition.	Derived from data in Hart et al. (2013)

ρ_S	–	0.10	Starvation body condition threshold	Derived from data in Hart et al. (2013)
ε^-	MJ·kg^{-1}	20-25	Catabolic efficiency of reserves conversion	See Appendix 1 text
ε^+	MJ·kg^{-1}	28-35	Anabolic efficiency of reserve conversion	Hin et al. (2019)
σ_L	–	0.86	Efficiency of conversion of mother's reserves to calf tissue	Lockyer (1993)
η	–	5-25	Steepness of assimilation response	See Appendix 1 text
γ	–	3	Shape parameter for effect of age on resource foraging efficiency	Hin et al. (2019)
T_R	days	0.75*T_L	Age at which calf's resource foraging efficiency is 50%	See Appendix 1 text
μ_s	-	0.05	Starvation mortality scalar	See Appendix 1 text
T_C	days	T_L/2	Calf age at which female begins to reduce milk supply	See Appendix 1 text
ξ_C	–	0.5	Non-linearity in milk assimilation-calf age relation	See Appendix 1 text
ξ_M	–	3-5	Non-linearity in female body condition-milk provisioning relation	See Appendix 1 text
φ_L	-	-	Lactation scalar	Calculated within DEB model

Gestation period (T_P): Generally considered to be 365 days (Perrin and Reilly, 1984), although slightly longer periods (range 355-395 days) have been recorded in captive animals (O'Brien and Robeck, 2012).

Lactation period/age at weaning (T_L): Perrin and Reilly (1984) report an average age at weaning of 18-20 months. The oldest nursing calf in their Table 7 was 38 months. A similar range (14-37 months) was recorded for captive animals by Kastelein et al. (2002). However, much higher ages at weaning (up to nine years) have been recorded for bottlenose dolphins in Shark Bay, Australia (Mann et al., 2000), where the modal age at weaning was over 40 months. We suggest using a range of 550-1000 days.

Structural length and structural mass ($L_0, L_\infty, \omega_1, \omega_2$)**:** Most published growth curves for bottlenose dolphins (e.g. Stolen et al., 2002; Neuenhoff et al., 2011; Bejarano et al., 2017) are not appropriate for UK bottlenose dolphin populations

because the maximum length obtained by UK animals is substantially greater than observed elsewhere. However, Cheney et al. (2018) fitted a Richard's growth curve:

$$L_a = L_\infty[1 - b.exp^{-ca}]^M \quad \text{Eq. A1}$$

to field measurements of known-age Moray Firth bottlenose dolphins using laser-photogrammetry, calibrated with data from stranded animals. L_a is length at age a, L_∞ is asymptotic length, b and c are free parameters that adjust the slope and inflection point of the curve, and M describes the position of the inflection point relative to the asymptote.

This curve could be used as the basis for a DEB model of UK bottlenose dolphins if it is combined with one of the formulae in Hart et al. (2013) that relate total mass to length for female bottlenose dolphins. Since we require an estimate of lean mass at age (Sa), the most appropriate formula is the one for emaciated animals:

$$S_a = 10^{-5.03}.L_a^{3.01} \quad \text{Eq. A2}$$

Field metabolic maintenance scalar (σ_M): Bejarano et al. (2017) considered three different approaches for calculating the daily Field Metabolic Rate (FMR) of bottlenose dolphins, primarily based on data collected in Sarasota Bay, Florida. These were: estimates based on the amount of energy consumed per day as a proportion of body mass for captive animals; a simple multiple of the Basal Metabolic Rate estimated from the Kleiber equation (i.e. σ_M) ; and direct measurements of daily FMR (expressed in MJ/kg) from free-ranging animals in summer and winter. Direct measurements of FMR in summer were 40% more than those made in winter. Summer water temperatures in the shallow waters of Sarasota Bay (mean 29.7℃) (Noren and Wells, 2009) are much higher than those likely to be encountered by bottlenose dolphins in UK waters, and so we suggest that the winter values are more appropriate for these populations. These winter field measurements predicted a daily FMR that was 4.5 – 6x (depending on the value used for metabolic mass - MMa) the value derived from the Kleiber equation, and we suggest that this provides a suitable range of values for use in a DEB model for UK bottlenose dolphins.

Energetic cost per unit structural mass (σ_G): We were unable to find any published estimates of the energy density of lean bottlenose dolphin tissue. We therefore suggest using the value of 30 $MJ.kg^{-1}$ that Hin et al. (2019) derived for pilot whales.

Relative cost of maintaining reserves (Θ_F): We were unable to find any published data that would allow a value specific to bottlenose dolphins to be calculated for this parameter. We therefore suggest using the value of 0.2 assumed by Hin et al. (2019).

Reserve thresholds (ρ, ρ_s): Bottlenose dolphins have a relatively thin blubber layer (thoracic blubber thickness 12-18 mm, based on Figure 2 of Noren and Wells, 2009), with an almost two-fold increase in estimated blubber mass between summer and winter for animals older than two years (Figure 3 in Noren and Wells, 2009). This suggests that blubber's main role in this species is to provide insulation rather than to act as an energy store.

A more realistic measure of reserve size can be derived from the difference in mass of dolphins of the same length. Ridgway and Fenner (1982) used data from 144 Atlantic bottlenose dolphins to calculate a length-specific ratio of weight:length that could be used to identify emaciated bottlenose dolphins. In a more extensive analysis of measurements from bottlenose dolphins in Sarasota Bay, Florida, Hart et al. (2013) fitted a set of equations for predicting mass from length. They suggested that the lower 95% quantile of this relationships (our Eq. A1) could be used to identify emaciated animals. Interestingly, the threshold weight:length ratios for emaciation predicted by this formula correspond closely with those suggested by Ridgway and Fenner (1982).

We have proposed using Equation A2 to estimate the structural mass of an individual at a given length. On this basis, the reserve mass of an individual can be estimated by subtracting its estimated structural mass from its actual weight. The upper 95% quantile of the Hart et al. (2013) relationship can be used to estimate the maximum expected values of body condition (ρt = reserve mass/total mass*).* Using these values, body condition varies from 0.272 for a 300 cm long animal to 0.335 for a 150 cm long individual. ρ*,* the target body condition, should be higher than any of these values, and we suggest 0.35. The equivalent range based on the median is 0.135-0.215. Because we have assumed that animals classified as emaciated using Hart et al. (2013) have no reserves, ρ_s (the starvation body condition threshold) is effectively 0.

Catabolic efficiency of reserve conversion (ε-): Results from studies of the weight loss of fasting pinnipeds and cetaceans, described in more detail in Section 4, indicate that catabolism of reserve tissue during these fasts generates 20-25 MJ for every kg lost. We suggest using this range of values for bottlenose dolphins.

Anabolic efficiency of reserve conversion ($\varepsilon+$): In the absence of any direct measurements of this parameter for bottlenose dolphins, we suggest following Hin et al. (2019) and using a range of values for $\varepsilon+$ that are 40% higher than ε- (i.e. 28-35 MJ.kg^{-1}).

Efficiency of conversion of mother's reserves to calf tissue (σ_L): In the absence of any direct measurements of the relevant efficiencies for bottlenose dolphins, we suggest using the value of 0.86 that was used by Hin et al. (2019).

Steepness of assimilation response (η): We were unable to find any data in the literature that could be used to set a feasible range for this parameter, and we suggest exploring the implications of values between 5 and 25.

Effect of age on resource foraging efficiency (γ, T_R): The majority of information on this parameter comes from studies of calves born in captivity. These animals are reported to begin feeding at age 6-18 months (Cockcroft and Ross, 1990; Peddemors et al., 1992; Kastelein et al., 2002). Mann and Smuts (1999) record that bottlenose dolphin calves in the Shark Bay, Australia population that are >3 months old "frequently" chase small fish and trap them at the water surface (a behaviour they call "snack foraging"), with the earliest observation of this behaviour occurring at 3 weeks. The quantity of food consumed by the calves studied by Kastelein et al. (2002) increased linearly over time, and stabilised before they were weaned. The latter effect is probably an artefact of captivity, because fish will be more difficult to catch in the wild. We suggest setting γ = 3, and T_R = 0.75*T_L.

Starvation-induced mortality rate (μ_s): Because of the way we have defined reserve thresholds, we need to modify the function used to calculate the daily starvation-induced mortality (see last line of Table 1 in Hin et al., 2019) to:

$$D_s(F, W) = -\mu_s \text{ if } F \leq 0 \qquad \text{Eq. A3}$$

Setting μ_s = 0.05 results in a 50% chance of survival if an emaciated animal is unable to assimilate enough energy to cover its daily energy costs for two weeks.

Pregnancy threshold ($F_{neonate}$): The pregnancy threshold determines when females become pregnant for the first time, and also whether or not females can become pregnant while lactating. Since the latter phenomenon is known to occur regularly in wild animals (e.g. Mann et al., 2000), it is important that the DEB can reproduce this and the formula used for $F_{neonate}$ should be tuned to achieve this and to match observed ages at first reproduction (e.g. from Perrin and Reilly, 1984).

Effect of calf age on milk assimilation (ξ_C, T_C): Again, most data on these parameters comes from captive animals. Most of the lactating females studied by Kastelein et al. (2002) dramatically increased their food intake shortly after parturition, and then slowly decreased it (although food intake remained above the maintenance level until calves were weaned). In contrast, the food intake levels of the four captive, lactating females studied by Reddy et al. (1994) remained at the same high level for 18 months. The DEB model is affected by both the calf's age and its body condition. As a result, calves that begin foraging early are predicted to demand less milk from their mothers than those that have not begun to forage. Thus, predicted milk assimilation may begin to decline before the calf is T_C days old. We suggest experimenting with values of T_C around $T_L/2$ and setting ξ_C = 0.5 (i.e. an almost linear decline in milk assimilation after age T_C).

Effect of female body condition on milk assimilation (ξ_M): Given the extended period of maternal care observed in bottlenose dolphin populations, females may be more willing to tolerate occasional large reductions in body condition during lactation than other species – such as harbour porpoise – that wean their calves at a relatively young age. This implies that higher values of this parameter, in the range of 3-5, may be most appropriate. However, the implications of lower values should be explored.

Lactation scalar (Φ_L) Once the basic equations of the DEB have been formulated, it will be possible to calculate a value for this parameter using the approach developed by Hin et al. (2019).

Appendix 2

Suggested parameter values for DEB models for minke whales

The suggested parameter values for minke whales are shown in Table 4, and details of how these parameters were derived are outlined below. These values should serve as a useful starting point for model development, but they will probably need to be refined as modelling progresses.

Table 4

Suggested parameter values for minke whales.

Symbol	Units	Value	Definition	Source
T_P	days	330	Gestation period	Perrin et al. (2018), but see Appendix 2 text
T_L	days	150	Age at weaning	Perrin et al. (2018)
L_0	cm	414.5	Length at "0" age	See Appendix 2 text
L_∞	cm	907	Maximum length	Christensen (1981)
k	$days^{-1}$	0.000389	Von Bertalanffy growth coefficient	Christensen (1981)
ω_1	$kg \cdot cm^{-1}$	0.0000362	Structural mass-length scaling constant	Hauksson et al. (2011)
ω_2	–	2.578	Structural mass-length scaling exponent	Hauksson et al. (2011)
K	$MJ \cdot kg^{-1}.day^{-1}$	0.294	Mass-specific Resting Metabolic Rate	Kleiber (1975)
σ_M	-	1.7-2.5	Field metabolic maintenance scalar	Folkow et al. (2000), but see Appendix 2 text
σ_G	$MJ \cdot kg^{-1}$	33	Energetic cost per unit structural mass	Calculated using the approach of Hin et al. (2019)
θ_F	–	0.2	Relative cost of maintaining reserves	Hin et al. (2019)
ρ	–	0.30	Target body condition.	See Appendix 2 text
ρ_S	–	0.10	Starvation body condition threshold	See Appendix 2 text
ε^-	$MJ \cdot kg^{-1}$	20-25	Catabolic efficiency of reserves conversion	See Appendix 2 text
ε^+	$MJ \cdot kg^{-1}$	28-35	Anabolic efficiency of reserve conversion	Hin et al. (2019)

σ_L	–	0.86	Efficiency of conversion of mother's reserves to calf tissue	Lockyer (1993)
η	–	5-25	Steepness of assimilation response	See Appendix 2 text
γ	–	3	Shape parameter for effect of age on resource foraging efficiency	Hin et al. (2019)
T_R	days	-	Age at which calf's resource foraging efficiency is 50%	See Appendix 2 text
μ_s	-	0.2	Starvation mortality scalar	Hin et al. (2019)
T_C	days	150	Calf age at which female begins to reduce milk supply	See Appendix 2 text
ξ_C	–	0	Non-linearity in milk assimilation-calf age relation	See Appendix 2 text
ξ_M	–	3-5	Non-linearity in female body condition-milk provisioning relation	See Appendix 2 text
φ_L	-	-	Lactation scalar	Calculated within DEB model

Gestation period (T_P): This is 10 months (~300 days) according to Perrin et al. (2018). However, a value of 330 days is more consistent with observed lengths at birth (see below).

Lactation period/age at weaning (T_L): This is 5-6 months according to Perrin et al. (2018). However, Nordøy et al. (1995) and Jonsgård (1951) report that minke whales spend 6 months in Northeast Atlantic waters each year and that calves are not normally seen with these animals. Given the reported annual breeding cycle of minke whales, this suggests that lactation must last less than six months and we suggest using a value of 150 days.

Structural length and structural mass $(L_0, L_\infty, \omega_1, \omega_2)$**:** A number of Van Bertalanffy growth curves have been published for the Central and Northeast Atlantic minke whale stocks (Christensen, 1981; Olsen and Sunde, 2002; Hauksson et al., 2011). However, none of these provide estimates of length at birth that are in the range 2.4-2.7 m reported by Perrin et al. (2018). Only the Christensen (1981) growth curve is consistent with Jonsgård (1951) suggestion that length at weaning is about 4.5 m. Hauksson et al. (2011) fitted the following growth curve for minke whale foetuses, based on animals sampled at the Icelandic whaling station:

$$L_t = 0.002 * t^{2.022}$$

where t is the age of the foetus in days. This predicts a length at birth of 2.04 m if gestation last 300 days, and 2.47 m if it is 330 days. We suggest modelling post-natal growth as linear from a length at birth of 2.47 m to 4.5 m at age T_L, and then using the Christensen (1981) growth curve (re-parameterised to match the formulation used by Hin et al. 2019):

$$L_a = 907.0 - 414.5e^{-0.000389a}$$

from this age onwards.

We suggest using the Hauksson et al. (2011) formula for the relationship between length and mass for foetuses to predict lean mass at age:

$$S_a = 3.62x10^{-2}.L_a^{2.758} \qquad \text{Equation A2.1}$$

Field metabolic maintenance scalar (σ_M): Blix and Folkow (1995) estimated the average energy expenditure of 6 free-ranging, tagged minke whales to be 80 kJ.kg^{-1}.day^{-1}, based on their respiration rate. Folkow et al. (2000) used this value to calculate that a 5,900 kg adult minke whale would expend 472 MJ.day^{-1}. This is equivalent to using a scalar of 1.7-2.5, depending on what assumptions are made about the values of ρ_t and Θ_F.

Energetic cost per unit structural mass (σ_G): We calculated growth efficiency using the same approach as Hin et al. (2019), with a mass at birth of 144 kg (based on a length at birth of 247 cm) and an energy density of 3.8 MJ.kg^{-1} for the tissue of minke whale foetuses estimated by Nordøy et al. (1995). This produced a value of 33 MJ.kg^{-1} for σ_G.

Relative cost of maintaining reserves (Θ_F): We were unable to find any published data that would allow a value specific to minke whales to be calculated for this parameter. We, therefore, suggest using the value of 0.2 assumed by Hin et al. (2019).

Reserve thresholds (ρ, ρ_s): Nordøy et al. (1995) provided detailed information on changes in the mass of blubber, muscle and intra-abdominal fat for immature and adult Northeast Atlantic minke whales, from the time they arrive on the feeding grounds (around 1 April) until their departure 180 days later. We combined this with information on the mean total weight of these animals and estimates of lean body

mass from Equation A2.1 to calculate a mean body condition of 0.14 for adult animals on arrival and of 0.25 when they depart. Based on the upper 95% confidence limit of the estimate of total mass for adult animals, we suggest that ρ should be set at 0.3. Adult females arriving on the feeding grounds will have just finished lactation and migration from their breeding grounds, so a body condition of 0.14 should represent a typical minimum level in their annual cycle. This suggests that 0.1 is an appropriate value for ρ_s.

Catabolic efficiency of reserve conversion (ε-): Results from studies of the weight loss of fasting cetaceans, described in more detail in Section 4, indicate that catabolism of reserve tissue during these fasts generates 20-25 MJ for every kg lost.

Anabolic efficiency of reserve conversion ($\varepsilon+$): In the absence of any direct measurements of this parameter for minke whales, we suggest following Hin et al. (2019) and using a range of values for $\varepsilon+$ that are 40% higher than ε- (i.e. 28-35 $MJ.kg^{-1}$).

Efficiency of conversion of mother's reserves to calf tissue (σ_L): In the absence of any direct measurements of the relevant efficiencies for minke whales, we suggest using the value of 0.86 that was used by Hin et al. (2019).

Steepness of assimilation response (η): We were unable to find any data in the literature that could be used to set a feasible range for this parameter, and we suggest exploring the implications of values between 5 and 25.

Effect of age on resource foraging efficiency (γ, T_R): We could find no information that could be used to estimate these parameters in the literature. We suggest experimenting with a range of values to ensure that most weaned calves are able to survive to breeding age.

Starvation-induced mortality rate (μ_s): No empirical information that could provide a species-specific value of this parameter for minke whales are available. As a starting point for exploratory modelling we suggest using the value of 0.2 used by Hin et al. (2019).

Pregnancy threshold ($F_{neonate}$): To achieve a one-year reproductive cycle, conception must occur early in lactation when females should be in good condition, because they will rely on their reserves to provide almost all of the energy required for lactation. During this time the energetic costs of gestation will be low. This suggests that $F_{neonate}$ should be set to a value that results in most mature females

becoming pregnant every year – as is observed in samples from the feeding grounds (Jonsgård, 1951).

Effect of calf age on milk assimilation (ξ_C, T_C): It is generally assumed that resource density is low on the breeding grounds and that females will provide almost all of their calves' energy requirements up to the age at weaning. We, therefore, suggest setting $T_C = T_L$.

Effect of female body condition on milk assimilation (ξ_M): Christiansen et al. (2014) found that foetal length-at-age in Icelandic minke whales was affected by maternal body condition. This suggests that female body condition may also affect milk assimilation and the effects of different values for ξ_M should be investigated.

Lactation scalar (Φ_L) Once the basic equations of the DEB have been formulated, it will be possible to calculate a value for this parameter using the approach developed by Hin et al. (2019).

Appendix 3

Suggested parameter values for DEB models for harbour seals

The suggested parameter values for harbour seals are shown in Table 5, and details of how these parameters were derived are outlined below. These values should serve as a useful starting point for model development, but they will probably need to be refined as modelling progresses.

Table 5

Suggested parameter values for harbour seals.

Symbol	Units	Value	Definition	Source
T_P	days	240	Gestation period	Reijnders et al. (1993)
T_L	days	40	Age at weaning	Sauve et al. (2014)
L_0	cm	82.9	Length at birth	Hall et al. (2019)
L_∞	cm	140.5	Maximum length	Hall et al. (2019)
k	$days^{-1}$	0.0012	Von Bertalanffy growth coefficient	Hall et al. (2019)
ω_1	$kg \cdot cm^{-1}$	0.000036	Structural mass-length scaling constant	Härkönen and Heide-Jørgensen (1990)
ω_2	–	2.874	Structural mass-length scaling exponent	Härkönen and Heide-Jørgensen (1990)
K	$MJ \cdot kg^{-1}.day^{-1}$	0.294	Mass-specific Resting Metabolic Rate	Kleiber (1975)
σ_M	-	3	Field metabolic maintenance scalar	See Appendix 3 text
σ_G	$MJ \cdot kg^{-1}$	25	Energetic cost per unit structural mass	Calculated using the approach of Hin et al. (2019)
θ_F	–	0.2	Relative cost of maintaining reserves	Hin et al. (2019)
ρ	–	0.43	Target body condition.	See Appendix 3 text
ρ_S	–	0.10	Starvation body condition threshold	See Appendix 3 text
ε^-	$MJ \cdot kg^{-1}$	20-25	Catabolic efficiency of reserves conversion	See Appendix 3 text
ε^+	$MJ \cdot kg^{-1}$	28-35	Anabolic efficiency of reserve conversion	Hin et al. (2019)

σ_L	–	0.86	Efficiency of conversion of mother's reserves to calf tissue	Lockyer (1993)
η	–	5-25	Steepness of assimilation response	See Appendix 3 text
γ	–	3	Shape parameter for effect of age on resource foraging efficiency	Hin et al. (2019)
T_R	days	100	Age at which calf's resource foraging efficiency is 50%	See Appendix 3 text
μ_s	-	0.2	Starvation mortality scalar	Hin et al. (2019)
T_C	days	24	Calf age at which female begins to reduce milk supply	Muelbert and Bowen (1993), but see Appendix 3 text
ξ_C	–	0.1	Non-linearity in milk assimilation-calf age relation	See Appendix 3 text
ξ_M	–	0.5-2.0	Non-linearity in female body condition-milk provisioning relation	See Appendix 3 text
φ_L	-	-	Lactation scalar	Calculated within DEB model

Gestation period (T_P): Generally considered to be around 320 days (10.5 months) including a 2-2.5 month period of diapause (Perrin and Reilly, 1984). We suggest using 240 days.

Lactation period/age at weaning (T_L): Around 3-6 weeks (Reijnders et al., 1993). Bowen et al. (2001) estimated a mean duration of 24 days, but Sauve et al. (2014) documented regular milk ingestion up to 40 days in known-age pups fitted with stomach temperature tags. This suggests that a value higher than 28 days may be appropriate.

Structural length and structural mass ($L_0, L_\infty, \omega_1, \omega_2$)**:** Hall et al. (2019) fitted Von Bertalanffy growth curves to age-at-length data for UK harbour seals. The growth curve for all females was:

$$L_a = 140.5 - 82.9e^{-0.0012a}$$

where *a* is age in days. Parameter values have been converted to match Hin et al.'s (2019) parameterisation of the Van Bertalanffy curve. The estimated age at birth is in the middle of the range (80-90 cm) reported by Reijnders et al. (1993).

Härkönen and Heide-Jørgensen (1990) estimated the following relationship between structural length and structural mass for harbour seals from the Baltic Sea:

$$S_a = 0.000036 L_a^{2.874}$$

Field metabolic maintenance scalar (σ_M): Although there are many estimates of the metabolic rate of harbour seals in captivity, we were unable to locate any field estimates. We, therefore, recommend using a value of three for this scalar exploring the effects of a range of values (see Appendix 4).

Energetic cost per unit structural mass (σ_G): We calculated growth efficiency using the same approach as Hin et al. (2019) and an energy density for harbour seal foetal tissue of 6.5 MJ.kg^{-1} (the mean of the values for newborn harp and grey seal pups reported by Worthy and Lavigne (1987)). This produced a value of 25 MJ.kg^{-1} for σ_G.

Relative cost of maintaining reserves (Θ_F): We were unable to find any published data that would allow a value specific to harbour seals to be calculated for this parameter. We, therefore, suggest using the value of 0.2 assumed by Hin et al. (2019).

Reserve thresholds (ρ, ρ_s): Unfortunately, we were unable to find any published estimates of variations in the body condition of free-ranging harbour seals over time. However, Härkönen and Heide-Jørgensen (1990) documented a decrease in the blubber thickness of adult female harbour seals in the Baltic from 36.7 mm at the start of lactation in May to 19 mm in August. This corresponded to a 26.5 kg reduction in an initial total mass of 72.4 kg. As a starting point for exploratory modelling, we suggest setting ρ_s to 0.1 and ρ to 0.43 at the start of lactation.

Catabolic efficiency of reserve conversion (ε-): Results from studies of the weight loss of fasting pinnipeds and cetaceans, described in more detail in Section 4, indicate that catabolism of reserve tissue during these fasts generates 20-25 MJ for every kg lost. We suggest using this range of values for harbour seals.

Anabolic efficiency of reserve conversion ($\varepsilon+$): In the absence of any direct measurements of this parameter for harbour seals, we suggest following Hin et al. (2019) and using a range of values for $\varepsilon+$ that are 40% higher than ε- (i.e. 28-35 MJ.kg^{-1}).

Efficiency of conversion of mother's reserves to calf tissue (σ_L): In the absence of any direct measurements of the relevant efficiencies for harbour seals, we suggest using the value of 0.86 that was used by Hin et al. (2019).

Steepness of assimilation response (η): We were unable to find any data in the literature that could be used to set a feasible range for this parameter, and we suggest exploring the implications of values between 5 and 25.

Effect of age on resource foraging efficiency (γ, T_R): Sauve et al. (2014) documented ingestion of solid food from day 14 in known-age pups fitted with stomach temperature tags. Muelbert and Bowen (1993) found that 80% of pups had begun feeding independently by age 50 days. However, these pups were all losing weight, indicating that their feeding efficiency was well below 100%. In the absence of any other information, we suggest setting T_R to 100 days and γ to three, which results in a foraging efficiency of 98% at age one year.

Starvation-induced mortality rate (μ_s): No empirical information that could provide a species-specific value of this parameter for harbour seals are available. As a starting point for exploratory modelling we suggest using the value of 0.2 used by Hin et al. (2019).

Pregnancy threshold ($F_{neonate}$): No empirical information that could provide a species-specific value of this parameter for harbour seals are available. We suggest setting $F_{neonate}$ to a value that results in most mature females becoming pregnant every year.

Effect of calf age on milk assimilation (ξ_C, T_C): Muelbert and Bowen (1993) estimated age at weaning as 24 days, based on the onset of weight loss in pups that were regularly weighed and the absence of milk in the stomach. However, Sauve et al. (2014) indicate that some milk is provided after this age. We therefore recommend setting T_C to 24 days and ξ_C to 0.1.

Effect of female body condition on milk assimilation (ξ_M): Bowen et al. (2001) documented a significant difference between the weight gain of pups born to harbour seal females whose weight ≤85 kg at the start of lactation and those born to females whose weight >85 kg. This suggests that female body condition may affect milk assimilation and that relative low values for ξ_M in the range 0.5-2.0 may be most appropriate for this species.

Lactation scalar (Φ_L) Once the basic equations of the DEB have been formulated, it will be possible to calculate a value for this parameter using the approach developed by Hin et al. (2019).

Appendix 4

Suggested parameter values for DEB models for grey seals

The suggested parameter values for grey seals are shown in Table 6, and details of how these parameters were derived are outlined below. These values should serve as a useful starting point for model development, but they will probably need to be refined as modelling progresses.

Table 6

Suggested parameter values for grey seals.

Symbol	Units	Value	Definition	Source
T_P	days	240	Gestation period	Hall and Russell (2018)
T_L	days	18	Age at weaning	Hall and Russell (2018)
L_0	cm	97.5	Length at birth	McLaren (1993)
L_∞	cm	184	Maximum length	McLaren (1993)
k	$days^{-1}$	0.0005	Von Bertalanffy growth coefficient	McLaren (1993), but see Appendix 4 text
ω_1	$kg \cdot cm^{-1}$	0.00001933	Structural mass-length scaling constant	Hauksson (2007)
ω_2	–	2.575	Structural mass-length scaling exponent	Hauksson (2007)
K	$MJ \cdot kg^{-1}.day^{-1}$	0.294	Mass-specific Resting Metabolic Rate	Kleiber (1975)
σ_M	-	2-3	Field metabolic maintenance scalar	See Appendix 4 text
σ_G	$MJ \cdot kg^{-1}$	25	Energetic cost per unit structural mass	Derived using the approach of Hin et al. (2019)
θ_F	–	0.2	Relative cost of maintaining reserves	Hin et al. (2019)
ρ	–	0.45	Target body condition.	See Appendix 4 text
ρ_S	–	0.10	Starvation body condition threshold	See Appendix 4 text
ε^-	$MJ \cdot kg^{-1}$	20-25	Catabolic efficiency of reserves conversion	See Appendix 4 text
ε^+	$MJ \cdot kg^{-1}$	28-35	Anabolic efficiency of reserve conversion	Hin et al. (2019)

σ_L	–	0.86	Efficiency of conversion of mother's reserves to calf tissue	Lockyer (1993)
η	–	5-25	Steepness of assimilation response	See Appendix 4 text
γ	–	3	Shape parameter for effect of age on resource foraging efficiency	See Appendix 4 text
T_R	days	150	Age at which calf's resource foraging efficiency is 50%	See Appendix 4 text
μ_s	-	0.2	Starvation mortality scalar	Hin et al. (2019)
T_C	days	T_L	Calf age at which female begins to reduce milk supply	See Appendix 4 text
ξ_C	–	0	Non-linearity in milk assimilation-calf age relation	See Appendix 4 text
ξ_M	–	-	Non-linearity in female body condition-milk provisioning relation	See Appendix 4 text
φ_L	-	-	Lactation scalar	Calculated within DEB model

Gestation period (T_P): Eight months (~ 240 days) according to Hall and Russell (2018).

Lactation period/age at weaning (T_L): Hall and Russell (2018) suggest the average age at weaning is 18 days.

Structural length and structural mass ($L_0, L_\infty, \omega_1, \omega_2$)**:** McLaren (1993) fitted this modified Von Bertalanffy growth curve to data from 527 female grey seals sampled at the Farne Islands:

$$L_a = \left(184.0 - e^{-(0.005(a+200.75))}\right)^{0.27}$$

where a is age in days. The estimated size at birth from this equation is 97.5 cm, which is within the range of 90-105 cm reported by Bonner (1981).

Boyd (1984) provided this linear growth equation for foetuses based on adult female seals collected at the Farne Islands:

$$L_a = 0.502a - 68.209$$

Hauksson (2007) estimated the following relationship between structural length and structural mass for grey seals from Iceland:

$$S_a = 0.0001933 L_a^{2.575}$$

Field metabolic maintenance scalar (σ_M): Sparling et al. (2006) measured the resting metabolic rate of captive adult and juvenile grey seals based on oxygen consumption and estimated that this was, on average, 1.95x that predicted by Kleiber's equation. Sparling and Fedak (2004) measured the Diving Metabolic Rate of captive grey seals and found that this was 1.7x that predicted by Kleiber's equation. They note that predictions of field metabolic rate of 2-3x the Kleiber value "*might be higher than they are in reality*". We suggest using values of both two and three for this parameter.

Energetic cost per unit structural mass (σ_G): We calculated growth efficiency using the same approach as Hin et al. (2019) and an energy density for foetal tissue of 6.5 MJ.kg^{-1} (the mean of the values for newborn harp and grey seal pups reported by Worthy and Lavigne (1987)). This produced a value of 25 MJ.kg^{-1} for σ_G.

Relative cost of maintaining reserves (Θ_F): We were unable to find any published data that would allow a value specific to grey seals to be calculated for this parameter. We, therefore, suggest using the value of 0.2 assumed by Hin et al. (2019).

Reserve thresholds (ρ, ρ_s): Boyd (1984) measured the total body weight and sculp (skin + blubber) weight of 72 adult female grey seals collected from the Farne Islands over the course of a year. Mean core weight did not vary over the year, once the weight of any foetus was accounted for. Total body weight was at a minimum at the end of lactation and did not begin to increase until after implantation of the embryo. Thereafter it increased to a maximum at the start of lactation. Pomeroy et al. (1999) documented a mean decline in weight of 67 kg over the course of lactation for females whose mean weight at the start of lactation was 185 kg. Lang et al. (2011) estimated that grey seal females utilize 50% of their energy reserves during lactation. We suggest that setting a value of 0.45 for ρ would be consistent with these values. This would result in female body condition declining to around 0.15 at the end of lactation, which would suggest a value of 0.1 for ρ_s. However, other values should be explored and model predictions of changes in body mass over the year and of the energy expended during lactation by females of different body sizes can be compared with the extensive literature on these variables in grey seals.

Catabolic efficiency of reserve conversion (ε-): Results from studies of the weight loss of fasting pinnipeds, described in more detail in Section 4, indicate that catabolism of reserve tissue during these fasts generates 20-25 MJ for every kg lost. We suggest using this range of values for grey seals.

Anabolic efficiency of reserve conversion (ε+): In the absence of any direct measurements of this parameter for grey seals, we suggest following Hin et al. (2019) and using a range of values for ε+ that are 40% higher than ε- (i.e. 28-35 $MJ.kg^{-1}$).

Efficiency of conversion of mother's reserves to calf tissue (σ_L): Lang et al. (2011) estimated that approximately 70% of the energy obtained by grey seal pups from milk was converted into tissue. However, this "storage efficiency" includes the costs of maintenance. We therefore suggest that the value of 0.86 which was used by Hin et al. (2019) is also appropriate for grey seals.

Steepness of assimilation response (η): We were unable to find any data in the literature that could be used to set a feasible range for this parameter, and we suggest exploring the implications of values between 5 and 25.

Effect of age on resource foraging efficiency (γ, T_R): Grey pups undertake a post-weaning fast of approximately 21 days (Noren et al., 2008). After this, they continue to lose weight for the next three months (Hall and McConnell, 2007) but regain their initial weight around the age of six months. We suggest setting T_R to 150 days and γ to three, which results in a very low foraging efficiency (<2%) up to age 40 days and 93.5% efficiency at age one year.

Starvation-induced mortality rate (μ_s): No empirical information that could provide a species-specific value of this parameter for grey seals are available. As a starting point for exploratory modelling we suggest using the value of 0.2 used by Hin et al. (2019).

Pregnancy threshold ($F_{neonate}$): Smout et al. (2019) documented a relationship between female mass at the end of lactation and likelihood of giving birth in the following breeding season. Given that females do not increase their body mass from the end of lactation until implantation (Boyd, 1984), information in Smout et al. (2019) for the body condition at the end of lactation for females that did give birth in the subsequent breeding season can be used to determine a preliminary value for $F_{neonate}$.

Effect of calf age on milk assimilation (ξ_C, T_C): There appears to be little variation in the amount of milk provided to the calf over the duration of lactation, suggesting that T_C should be identical to T_L.

Effect of female body condition on milk assimilation (ξ_M): It should be possible to estimate this parameter from data on the effect of female post-partum mass on pup mass at weaning (Pomeroy et al., 1999; Bowen et al., 2006) and the mean rate of milk delivery.

Lactation scalar (Φ_L) Once the basic equations of the DEB have been formulated, it will be possible to calculate a value for this parameter using the approach developed by Hin et al. (2019).

References

Arso Civil, M., B. Cheney, N. J. Quick, V. Islas-Villanueva, J. A. Graves, V. M. Janik, P. M. Thompson, and P. S. Hammond. 2018. Variations in age-and sex-specific survival rates help explain population trend in a discrete marine mammal population. Ecology and Evolution

Bejarano, A. C., R. S. Wells, and D. P. Costa. 2017. Development of a bioenergetic model for estimating energy requirements and prey biomass consumption of the bottlenose dolphin Tursiops truncatus. Ecological Modelling 356:162-172.

Beltran, R. S., J. W. Testa, and J. M. Burns. 2017. An agent-based bioenergetics model for predicting impacts of environmental change on a top marine predator, the Weddell seal. Ecological Modelling 351:36-50.

Bennett, K. A., J. R. Speakman, S. E. Moss, P. Pomeroy, and M. A. Fedak. 2007. Effects of mass and body composition on fasting fuel utilisation in grey seal pups (Halichoerus grypus Fabricius): an experimental study using supplementary feeding. Journal of Experimental Biology 210(17):3043-3053.

Blix, A., and L. Folkow. 1995. Daily energy expenditure in free living minke whales. Acta Physiologica 153(1):61-66.

Bonner, W. 1981. Grey Seal *Halichoerus grypus Fabricius*, 1791., Ridgway, S.H. & Harrison, R.J. (eds.) Handbook of Marine Mammals Volume 2 Seals. Academic Press, London. p. Pp 111-144.

Booth, C. G. 2020. Food for thought: Harbor porpoise foraging behavior and diet inform vulnerability to disturbance. Marine Mammal Science doi: https://doi.org/10.1111/mms.12632

Booth, C. G., F. Heinis, and H. J. 2019. Updating the Interim PCoD Model: Workshop Report - New transfer functions for the effects of disturbance on vital rates in marine mammal species, Report Code SMRUC-BEI-2018-011, submitted to the Department for Business, Energy and Industrial Strategy (BEIS), February 2019 (unpublished).

Bowen, W., S. J. Iverson, J. McMillan, and D. Boness. 2006. Reproductive performance in grey seals: age-related improvement and senescence in a capital breeder. Journal of Animal Ecology 75(6):1340-1351.

Bowen, W. D., S. L. Ellis, S. J. Iverson, and D. J. Boness. 2001. Maternal effects on offspring growth rate and weaning mass in harbour seals. Canadian Journal of Zoology 79(6):1088-1101.

Boyd, I. 1984. The relationship between body condition and the timing of implantation in pregnant grey seals (Halichoerus grypus). Journal of Zoology 203(1):113-123.

Braithwaite, J. E., J. J. Meeuwig, and M. R. Hipsey. 2015. Optimal migration energetics of humpback whales and the implications of disturbance. Conservation Physiology 3(1):cov001. doi: 10.1093/conphys/cov001

Brody, S. 1968. Bioenergetics and growth, revised 1945 edn. Hafner Publishing, New York, NY.

Cheney, B., R. Wells, T. Barton, and P. Thompson. 2018. Laser photogrammetry reveals variation in growth and early survival in free-ranging bottlenose dolphins. Animal Conservation 21(3):252-261.

Christensen, I. 1981. Age determination of minke whales, Balaenoptera acutorostrata, from laminated structures in the tympanic bullae. Rep. int. Whal. Commn. 31:245-253.

Christiansen, F., and D. Lusseau. 2015. Linking Behavior to Vital Rates to Measure the Effects of Non-Lethal Disturbance on Wildlife. Conservation Letters 8(6):424-431.

Christiansen, F., G. A. Víkingsson, M. H. Rasmussen, and D. Lusseau. 2014. Female body condition affects foetal growth in a capital breeding mysticete. Functional ecology 28(3):579-588.

Cockcroft, V., and G. Ross. 1990. Observations on the early development of a captive bottlenose dolphin calf. The bottlenose dolphin 461:478.

Costa, D., B. L. Boeuf, A. Huntley, and C. Ortiz. 1986. The energetics of lactation in the northern elephant seal, Mirounga angustirostris. Journal of Zoology 209(1):21-33.

De Roos, A. M., N. Galic, and H. Heesterbeek. 2009. How resource competition shapes individual life history for nonplastic growth: ungulates in seasonal food environments. Ecology 90(4):945-960.

Farmer, N. A., D. P. Noren, E. M. Fougères, A. Machernis, and K. Baker. 2018. Resilience of the endangered sperm whale Physeter macrocephalus to foraging disturbance in the Gulf of Mexico, USA: a bioenergetic approach. Marine Ecology Progress Series 589:241-261.

Folkow, L. P., T. Haug, K. T. Nilssen, and E. S. Nordøy. 2000. Estimated food consumption of minke whales Balaenoptera acutorostrata in Northeast Atlantic waters in 1992-1995. NAMMCO Sci. Publ 2:65-80.

Gallagher, C. A., S. J. Stern, and E. Hines. 2018. The metabolic cost of swimming and reproduction in harbor porpoises (Phocoena phocoena) as predicted by a bioenergetic model. Marine Mammal Science online viewingdoi: 10.1111/mms.12487

Gaskin, D. 1984. The harbour porpoise *Phocoena phocoena* (L.): regional populations, status, and information on direct and indirect catches, Report to the International Whaling Commission.

Goedegebuure, M. 2018. Improving representations of higher trophic-level species in models: using individual-based modelling and dynamic energy budget theory to project population trajectories of southern elephant seals, University of Tasmania.

Goedegebuure, M., J. Melbourne-Thomas, S. P. Corney, C. R. McMahon, and M. A. Hindell. 2018. Modelling southern elephant seals Mirounga leonina using an individual-based model coupled with a dynamic energy budget. PloS one 13(3):e0194950.

Hall, A., B. Mackey, J. Kershaw, and P. Thompson. 2019. Age–length relationships in UK harbour seals during a period of population decline. Aquatic Conservation Marine and Freshwater Ecosystems. 29(S1):61-70.

Hall, A. J., and B. J. McConnell. 2007. Measuring changes in juvenile gray seal body composition. Marine Mammal Science 23(3):650-665.

Hall, A. J., and D. J. Russell. 2018. Gray Seal: Halichoerus grypus, Encyclopedia of marine mammals. Elsevier. p. 420-422.

Härkönen, T., and M.-P. Heide-Jørgensen. 1990. Comparative life histories of East Atlantic and other harbour seal populations. Ophelia 32(3):211-235.

Hart, L. B., R. S. Wells, and L. H. Schwacke. 2013. Reference ranges for body condition in wild bottlenose dolphins *Tursiops truncatus*. Aquatic Biology 18(1):63-68.

Harwood, J., C. G. Booth, and D. Tollit. 2019. Walrus Interim PCoD Model: Workshop Report - New transfer functions for the effects of acoustic disturbance on vital rates in Pacific Walrus. US Fish and Wildlife Service, Anchorage. US Fish and Wildlife Service, Anchorage.

Hauksson, E. 2007. Growth and reproduction in the Icelandic grey seal. NAMMCO Scientific Publications 6:153-162.

Hauksson, E., G. Vikingsson, S. Halldorsson, D. Olafsdottir, and J. Sigurjonsson. 2011. Preliminary report on biological parameters for North Atlanicminke whales in Icelandic waters, IWC 2011 SC/63/O15.

Hin, V., J. Harwood, and A. M. de Roos. 2019. Bio-energetic modeling of medium-sized cetaceans shows high sensitivity to disturbance in seasons of low resource supply. Ecological Applications:e01903.

Hin, V., J. Harwood, and A. M. De Roos. in review. How density-dependent processes hide the population consequences of disturbance. Journal of Animal Ecology TBC(TBC):TBC.

Jager, T., E. Ravagnan, and S. Dupont. 2016. Near-future ocean acidification impacts maintenance costs in sea-urchin larvae: identification of stress factors and tipping points using a DEB modelling approach. Journal of Experimental Marine Biology and Ecology 474:11-17.

Jonsgård, Å. 1951. Studies on the Little Piked Whale Or Minke Whale (Balaenoptera Acuto-rostrata Lacépède): Report on Norwegian Investigations Carried Out in the Years 1943-1950. OEEC.

Kastelein, R., N. Vaughan, S. Walton, and P. Wiepkema. 2002. Food intake and body measurements of Atlantic bottlenose dolphins (Tursiops truncates) in captivity. Marine Environmental Research 53(2):199-218.

Kastelein, R. A., L. Helder-Hoek, and N. Jennings. 2018. Seasonal Changes in Food Consumption, Respiration Rate, and Body Condition of a Male Harbor Porpoise (*Phocoena phocoena*). Aquatic Mammals 44(1):76-91.

Kastelein, R. A., L. Helder-Hoek, N. Jennings, R. van Kester, and R. Huisman. 2019. Reduction in body mass and blubber thickness of harbor porpoises (Phocoena phocoena) due to near-fasting for 24 hours in four seasons. Aquatic Mammals 45(1):37-47.

Kastelein, R. A., and R. Van Battum. 1990. The relationship between body weight and morphological measurements in harbour porpoises (Phocoena phocoena) from the North Sea. Aquat Mamm 16:48-52.

Klanjscek, T., R. M. Nisbet, H. Caswell, and M. G. Neubert. 2007. A model for energetics and bioaccumulation in marine mammals with applications to the right whale. Ecological Applications 17(8):2233-2250.

Kleiber, M. 1975. The fire of life. Robert E. Kreiger, New York

Kooijman, B., and S. Kooijman. 2010. Dynamic energy budget theory for metabolic organisation. Cambridge university press.

Koopman, H. N. 2007. Phylogenetic, ecological, and ontogenetic factors influencing the biochemical structure of the blubber of odontocetes. Marine Biology 151(1):277-291.

Koopman, H. N., D. A. Pabst, W. A. Mclellan, R. Dillaman, and A. Read. 2002. Changes in blubber distribution and morphology associated with starvation in the harbor porpoise (Phocoena phocoena): evidence for regional differences in blubber structure and function. Physiological and Biochemical Zoology 75(5):498-512.

Lang, S. L. C., S. J. Iverson, and W. D. Bowen. 2011. The Influence of Reproductive Experience on Milk Energy Output and Lactation Performance in the Grey Seal (*Halichoerus grypus*). PLoS ONE 6(5)

Learmonth, J. A., S. Murphy, P. L. Luque, R. J. Reid, I. A. P. Patterson, A. Brownlow, H. M. Ross, J. P. Barley, M. Begona Santos, and G. J. Pierce. 2014. Life history of harbor porpoises (*Phocoena phocoena*) in Scottish (UK) waters. Marine Mammal Science 30(4):1427-1455.

Lockyer, C. 1993. Seasonal changes in body fat condition of northeast Atlantic pilot whales, and their biological significance. IWC Special Issue 14: Biology of the Northern Hemisphere Pilot Whales:205-324.

Lockyer, C. 2003. Harbour porpoises (*Phocoena phocoena*) in the North Atlantic: Biological parameters. NAMMCO Scientific Publications 5:71-89.

Lockyer, C. 2007. All creatures great and smaller: a study in cetacean life history energetics. Journal of the Marine Biological Association of the United Kingdom 87(4):1035-1045. doi: 10.1017/S0025315407054720

Lockyer, C., M. Heide-Jørgensen, J. Jensen, and M. Walton. 2003. Life history and ecology of harbour porpoises (*Phocoena phocoena*) from West Greenland. NAMMCO Scientific Publications 5:177-194.

Lockyer, C., and C. Kinze. 2003. Status, ecology and life history of harbour porpoise (*Phocoena phocoena*), in Danish waters. 2003 5:33. (harbour porpoises;status;ecology;life history) doi: 10.7557/3.2745

Mann, J., R. C. Connor, L. M. Barre, and M. R. Heithaus. 2000. Female reproductive success in bottlenose dolphins (Tursiops sp.): life history, habitat, provisioning, and group-size effects. Behavioral Ecology 11(2):210-219.

Mann, J., and B. Smuts. 1999. Behavioral development in wild bottlenose dolphin newborns (Tursiops sp.). Behaviour 136(5):529-566.

McHuron, E. A., D. P. Costa, L. Schwarz, and M. Mangel. 2016. State-dependent behavioural theory for assessing the fitness consequences of anthropogenic disturbance on capital and income breeders. Methods in Ecology and Evolution:n/a-n/a. doi: 10.1111/2041-210X.12701

McHuron, E. A., M. Mangel, L. K. Schwarz, and D. P. Costa. 2017. Energy and prey requirements of California sea lions under variable environmental conditions. Marine Ecology Progress Series 567:235-247.

McHuron, E. A., L. K. Schwarz, D. P. Costa, and M. Mangel. 2018. A state-dependent model for assessing the population consequences of disturbance on income-breeding mammals. Ecological modelling 385:133-144.

McLaren, I. 1993. Growth in pinnipeds. Biological Reviews 68(1):1-79.

McLellan, W. A., H. N. Koopman, S. Rommel, A. Read, C. Potter, J. Nicolas, A. J. Westgate, and D. A. Pabst. 2002. Ontogenetic allometry and body composition of harbour porpoises (Phocoena phocoena, L.) from the western North Atlantic. Journal of Zoology 257(4):457-471.

Møhl-Hansen, U. 1954. Investigations on reproduction and growth of the porpoise (Phocaena phocaena (L.)) from the Baltic. Vidensk. Meddr. Dansk naturh. Foren 116:369-396.

Moretti, D. 2019. Determining the effect of Mid-Frequency Active (MFA) sonar on fitness of Blainville's beaked whales (*Mesoplodon densirostris*) in the Tongue of the Ocean., University of St Andrews.

Muelbert, M., and W. Bowen. 1993. Duration of lactation and postweaning changes in mass and body composition of harbour seal, Phoca vitulina, pups. Canadian Journal of zoology 71(7):1405-1414.

Murphy, C. A., R. M. Nisbet, P. Antczak, N. Garcia-Reyero, A. Gergs, K. Lika, T. Mathews, E. B. Muller, D. Nacci, and A. Peace. 2018a. Linking adverse outcome pathways to dynamic energy budgets: A conceptual model, A Systems Biology Approach to Advancing Adverse Outcome Pathways for Risk Assessment. Springer. p. 281-302.

Murphy, C. A., R. M. Nisbet, P. Antczak, N. Garcia-Reyero, A. Gergs, K. Lika, T. Mathews, E. B. Muller, D. Nacci, and A. Peace. 2018b. Incorporating suborganismal processes into dynamic energy budget models for ecological risk assessment. Integrated environmental assessment and management 14(5):615-624.

Nabe-Nielsen, J., R. M. Sibly, J. Tougaard, J. Teilmann, and S. Sveegaard. 2014. Effects of noise and by-catch on a Danish harbour porpoise population. Ecological Modelling 272:242-251.

Nabe-Nielsen, J., F. van Beest, V. Grimm, R. Sibly, J. Teilmann, and P. M. Thompson. 2018. Predicting the impacts of anthropogenic disturbances on marine populations. Conservation Letters e12563

National Academies of Sciences Engineering and Medicine. 2017. Approaches to Understanding the Cumulative Effects of Stressors on Marine Mammals, Washington, DC: The National Academies Press.

Neuenhoff, R. D., D. F. Cowan, H. Whitehead, and C. D. Marshall. 2011. Prenatal data impacts common bottlenose dolphin (T*ursiops truncatus*) growth parameters estimated by length-at-age curves. Marine Mammal Science 27(1):195-216.

New, L. F., J. S. Clark, D. P. Costa, E. Fleishman, M. Hindell, T. Klanjšček, D. Lusseau, S. Kraus, C. McMahon, and P. Robinson. 2014. Using short-term measures of behaviour to estimate long-term fitness of southern elephant seals. Marine Ecology Progress Series 496:99-108.

New, L. F., D. J. Moretti, S. K. Hooker, D. P. Costa, and S. E. Simmons. 2013. Using Energetic Models to Investigate the Survival and Reproduction of Beaked Whales (family Ziphiidae). PLoS ONE 8(7)

Nisbet, R., E. Muller, K. Lika, and S. Kooijman. 2000. From molecules to ecosystems through dynamic energy budget models. Journal of animal ecology 69(6):913-926.

Nordøy, E., L. Folkow, P. Mårtensson, and A. Blix. 1995. Food requirements of Northeast Atlantic minke whales. Whales, Seals, Fish and Man. AS Blix, L. Walløe, and Ø. Ulltang (eds.). Dev. Mar. Bio 4:307-317.

Noren, D., D. Crocker, T. Williams, and D. Costa. 2003. Energy reserve utilization in northern elephant seal (Mirounga angustirostris) pups during the postweaning fast: size does matter. Journal of Comparative Physiology B 173(5):443-454.

Noren, D. P. 2011. Estimated field metabolic rates and prey requirements of resident killer whales. Marine Mammal Science 27(1):60-77.

Noren, S. R., D. J. Boness, S. J. Iverson, J. McMillan, and W. D. Bowen. 2008. Body condition at weaning affects the duration of the postweaning fast in gray seal pups (Halichoerus grypus). Physiological and Biochemical Zoology 81(3):269-277.

Noren, S. R., M. S. Udevitz, and C. V. Jay. 2014. Energy Demands for Maintenance, Growth, Pregnancy, and Lactation of Female Pacific Walruses.

Noren, S. R., and R. S. Wells. 2009. Blubber deposition during ontogeny in free-ranging bottlenose dolphins: balancing disparate roles of insulation and locomotion. Journal of Mammalogy 90(3):629-637.

O'Brien, J. K., and T. R. Robeck. 2012. The relationship of maternal characteristics and circulating progesterone concentrations with reproductive outcome in the bottlenose dolphin (*Tursiops truncatus*) after artificial insemination, with and without ovulation induction, and natural breeding. Theriogenology 78(3):469-482.

Olsen, E., and J. Sunde. 2002. Age determination of minke whales (Balaenoptera acutorostrata) using the aspartic acid racemization technique. Sarsia 87(1):1-8.

Peddemors, V., M. Fothergill, and V. Cockcroft. 1992. Feeding and growth in a captive-born bottlenose dolphin Tursiops truncatus. African Zoology 27(2):74-80.

Perrin, W. F., S. D. Mallette, and R. L. Brownell Jr. 2018. Minke whales: Balaenoptera acutorostrata and B. bonaerensis, Encyclopedia of marine mammals. Elsevier. p. 608-613.

Perrin, W. F., and S. B. Reilly. 1984. Reproductive parameters of dolphins and small whales of the family Delphinidae. Report of the International Whaling Commission (Special Issue 6):97-133.

Pirotta, E., C. G. Booth, D. P. Costa, E. Fleishman, S. D. Kraus, D. Lusseau, D. Moretti, L. F. New, R. S. Schick, and L. K. Schwarz. 2018a. Understanding the population consequences of disturbance. Ecology and Evolution doi: https://onlinelibrary.wiley.com/doi/full/10.1002/ece3.4458

Pirotta, E., V. Hin, M. Mangel, L. New, D. P. Costa, A. M. de Roos, and J. Harwood. in Review. Propensity for risk in reproductive strategy affects susceptibility to anthropogenic disturbance. American Naturalist

Pirotta, E., M. Mangel, D. P. Costa, J. Goldbogen, J. Harwood, V. Hin, L. M. Irvine, B. R. Mate, E. A. McHuron, and D. M. Palacios. 2019. Anthropogenic disturbance in a changing environment: modelling lifetime reproductive success to predict the consequences of multiple stressors on a migratory population. Oikos

Pirotta, E., M. Mangel, D. P. Costa, B. Mate, J. A. Goldbogen, D. M. Palacios, L. A. Hückstädt, E. A. McHuron, L. Schwarz, and L. New. 2018b. A Dynamic State

Model of Migratory Behavior and Physiology to Assess the Consequences of Environmental Variation and Anthropogenic Disturbance on Marine Vertebrates. The American Naturalist 191(2):E000-E000.

Pirotta, E., L. K. Schwarz, D. P. Costa, P. W. Robinson, and L. New. 2018c. Modeling the functional link between movement, feeding activity, and condition in a marine predator. Behavioral Ecology 30(2):434-445. doi: 10.1093/beheco/ary183

Pomeroy, P., M. Fedak, P. Rothery, and S. Anderson. 1999. Consequences of maternal size for reproductive expenditure and pupping success of grey seals at North Rona, Scotland. Journal of Animal Ecology 68(2):235-253.

Read, A. J. 1990. Estimation of body condition in harbour porpoises, Phocoena phocoena. Canadian Journal of Zoology 68(9):1962-1966.

Read, A. J., and K. A. Tolley. 1997. Postnatal growth and allometry of harbour porpoises from the Bay of Fundy. Canadian Journal of Zoology 75(1):122-130.

Reddy, M., T. Kamolnick, C. Curry, D. Skaar, and S. Ridgway. 1994. Energy requirements for the bottlenose dolphin (Tursiops truncatus) in relation to sex, age and reproductive status. Marine Mammals: Public Display and Research 1(1):26-31.

Reijnders, P., S. Brasseur, J. van der Toorn, P. van der Wolf, I. Boyd, J. Harwood, D. Lavigne, and L. Lowry. 1993. Seals, fur seals, sea lions, and walrus. Status survey and conservation action plan. IUCN The World Conservation Union.

Richardson, S., G. Stenson, and C. Hood. 2003. Growth of the harbour porpoise (Phocoena phocoena) in eastern Newfoundland, Canada. NAMMCO Scientific Publications 5:211-221.

Ridgway, S., and C. Fenner. 1982. Weight-length relationships of wild-caught and captive Atlantic bottlenose dolphins. Journal of the American Veterinary Medical Association 181(11):1310-1315.

Sauve, C. C., J. Van de Walle, M. O. Hammill, J. P. Arnould, and G. Beauplet. 2014. Stomach temperature records reveal nursing behaviour and transition to solid food consumption in an unweaned mammal, the harbour seal pup (Phoca vitulina). PLoS one 9(2)

Schick, R. S., L. F. New, L. Thomas, D. P. Costa, M. A. Hindell, C. R. McMahon, P. W. Robinson, S. E. Simmons, M. Thums, and J. Harwood. 2013. Estimating resource acquisition and at-sea body condition of a marine predator. Journal of animal ecology 82(6):1300-1315.

Sinclair, R., J. Harwood, and C. Sparling. 2020. Review of demographic parameters and sensitivity analysis to inform inputs and outputs of population consequences of disturbance assessments for marine mammals, Report number SMRUC-MSC-2019-004 provided to Marine Scotland.

Smout, S., R. King, and P. Pomeroy. 2019. Environment-sensitive mass changes influence breeding frequency in a capital breeding marine top predator. Journal of Animal Ecology

Sparling, C. E., and M. A. Fedak. 2004. Metabolic rates of captive grey seals during voluntary diving. Journal of Experimental Biology 207(10):1615-1624.

Sparling, C. E., J. R. Speakman, and M. A. Fedak. 2006. Seasonal variation in the metabolic rate and body composition of female grey seals: fat conservation prior to high-cost reproduction in a capital breeder? Journal of Comparative Physiology B 176(6):505-512.

Spitz, J., V. Ridoux, A. W. Trites, S. Laran, and M. Authier. 2018. Prey consumption by cetaceans reveals the importance of energy-rich food webs in the Bay of Biscay. Progress in Oceanography 166:148-158. doi: https://doi.org/10.1016/j.pocean.2017.09.013

Srinivasan, M., T. M. Swannack, W. E. Grant, J. Rajan, and B. Würsig. 2018. To feed or not to feed? Bioenergetic impacts of fear-driven behaviors in lactating dolphins. Ecology and Evolution

Stolen, M. K., D. K. Odell, and N. B. Barros. 2002. Growth of bottlenose dolphins (Tursiops truncatus) from the Indian River Lagoon system, Florida, USA. Marine Mammal Science 18(2):348-357.

Villegas-Amtmann, S., L. Schwarz, G. Gailey, O. Sychenko, and D. Costa. 2017. East or west: the energetic cost of being a gray whale and the consequence of losing energy to disturbance. Endangered Species Research 34:167-183.

Villegas-Amtmann, S., L. Schwarz, J. Sumich, and D. Costa. 2015. A bioenergetics model to evaluate demographic consequences of disturbance in marine mammals applied to gray whales. Ecosphere 6(10):1-19.

Winship, A. 2009. Estimating the impact of bycatch and calculating bycatch limits to achieve conservation objectives as applied to harbour porpoise in the North Sea, University of St Andrews.

Worthy, G. A., and D. Lavigne. 1987. Mass loss, metabolic rate, and energy utilization by harp and gray seal pups during the postweaning fast. Physiological Zoology 60(3):352-364.

Marine Scotland Science
Marine Laboratory
375 Victoria Road
Aberdeen
AB11 9DB

Copies of this report are available from the Marine Scotland website at
www.gov.scot/marinescotland